PALEOLIQUEFACTION STUDY IN THE CENTRAL VIRGINIA SEISMIC ZONE AND SURROUNDING REGION

Final Technical Report

Research supported by the U.S. Geological Survey (USGS),
Department of the Interior, under USGS grant G18AP00027

Principal Investigator
Martitia P. Tuttle
M. Tuttle & Associates
128 Tibbetts Lane
Georgetown, ME 04548
Tel: 207-371-2007
E-mail: mptuttle@earthlink.net
URL: http://www.mptuttle.com

Project Period: 4/1/2018-12/31/2019

Program Element I: National and Regional Earthquake Hazards Assessments

Key Words: Paleoliquefaction, Paleoseismology, Age Dating

PALEOLIQUEFACTION STUDY IN THE CENTRAL VIRGINIA SEISMIC ZONE AND SURROUNDING REGION

Principal Investigator
Martitia P. Tuttle

Report Contributors
Kathleen Dyer-Williams
and Kathleen Tucker

M. Tuttle & Associates
P.O. Box 345
Georgetown, ME 04548
Tel: 207-371-2007
E-mail: mptuttle@earthlink.net

Abstract

During surveys along 69 km of the Mattaponi and Pamunkey Rivers in the eastern portion of the Central Virginia seismic zone, thirteen earthquake-induced liquefaction features were discovered at six sites. No earthquake-induced liquefaction features were found during survey along 8 km of the James River in the southern portion of the seismic zone. Based on these findings and those from our previous study in 2015, there are at least two generations of liquefaction features that formed in the Central Virginia seismic zone prior to the 2011 **M** 5.7 Mineral earthquake. The younger generation of liquefaction features exhibits relatively little iron staining or mottling and likely formed during the past 350 years. They are small (dikes ≤ 3 cm wide), few in number, and appear to be limited in distribution to the James and Pamunkey Rivers. The 1875 **M** 4.8 ± 0.2 (MMI VII), earthquake thought to be located northwest of Goochland, is the largest historical event to strike the area and the likely cause of the historic liquefaction features. According to the relation between earthquake magnitude and distance to liquefaction, however, the 1875 earthquake would have to be of greater magnitude or located closer to the James and Pamunkey sites to induce liquefaction there. The older generation of liquefaction features exhibits bioturbation and mottling and likely formed between 350 and 2800 years ago. They are larger, more numerous, and more broadly distributed, including along the Mattaponi, Pamunkey, South Ann, and Rivanna Rivers, than the younger generation. The largest paleoliquefaction features, dikes up to 20 cm wide, occur on the Pamunkey and Mattaponi Rivers, suggesting that the earthquake source may be located nearby, perhaps in the Ashland area where a cluster of small earthquakes have been recorded since 1974. According to the magnitude-distance relation, a **M** ≥ 6.5 paleoearthquake centered near Ashland could explain the larger liquefaction features along the Mattaponi and Pamunkey Rivers as well as the regional distribution. Evaluation of scenario earthquakes using liquefaction potential analysis, found that a **M** 6.75 produced by a source near Ashland would induce liquefaction at sites along the Mattaponi, Pamunkey, South Anna, and Rivanna Rivers. Alternatively, a **M** 6.25 earthquake produced by the Mineral source and a **M** 6.0 earthquake produced by a source near Ashland also could explain the regional distribution of paleoliquefaction features, but would not account for the larger size of features along the Mattaponi and Pamunkey Rivers.

Introduction

On August 23, 2011, a moment magnitude, **M**, 5.7 ± 0.1 earthquake occurred near Mineral, Virginia about 50 km east of Charlottesville, 60 km northwest of Richmond, and 130 km southwest of Washington, D.C. (Figures 1 and 2; Horton et al., 2015). The m_{bLg} (magnitude derived from the displacement amplitude of Lg waves) of the earthquake was 6.28 ± 0.26 (Chapman, 2015). The earthquake was felt along most of the eastern seaboard from Georgia to Canada. It caused damage to residences, buildings, schools, and earthen dams in the epicentral area as well as to bridges, prominent buildings, and monuments in Washington, D.C. (Horton et al., 2015). Minor damage was reported as far away as New Jersey, New York, and South Carolina. Peak ground acceleration (PGA) of 0.27 g, measured 23 km northeast of the epicenter at the North Anna nuclear power plant, was greater than the 2% probability of exceedance for hard rock shown on the seismic hazard maps for the central Virginia seismic zone (CVSZ) (Petersen et al., 2008). The mainshock and some aftershocks were characterized by high stress drops in the 50-100 MPa range, comparable to those of the 1988 **M** 5.9 Saguenay, Canada, 2010 **M** 7.1 Darfield, New Zealand, and 2011 **M** 6.3 Christchurch, New Zealand, earthquakes (Ellsworth et al., 2011).

The 2011 Mineral earthquake occurred in the CVSZ, an area of diffuse seismicity with most earthquakes occurring within ~60 km of the James River between Richmond and Charlottsville (Figure 1; e.g., Chapman, 2015). The estimated return period for $m_{bLg} \geq 6.3$ earthquakes, like the 2011 Mineral event, is 752 yr, with a 95% confidence interval of 385-1471 yr (Chapman, 2015). Seismicity in the CVSZ ranges in depth from near surface to 12 km (Bollinger et al., 1985). Because the southern Appalachian detachment is at least 12 km deep in this part of the Piedmont, seismicity of the CVSZ is thought to occur on the Paleozoic and Mesozoic faults above the Precambrian basement though there is no clear association with any particular mapped fault (e.g., Pratt et al., 1988 and 2015; Chapman, 2015).

The 2011 Mineral earthquake is thought to be the result of reverse slip on a northeast-trending, southeast-dipping fault in the Eastern Piedmont thrust sheet and within a belt of Triassic basins associated with rifting and opening of the Atlantic Ocean (Ellsworth et al., 2011). The mainshock and more than thirty aftershocks of $\mathbf{M} \leq 4.5$ occurred in Ordovician volcanogenic and intrusive rocks of the Chopawamsic terrane northwest of the late Paleozoic, dextral strike-slip Spotsylvania fault zone and southeast of the early Paleozoic Chopawamsic thrust fault (Figure 2; Horton et al., 2015; Powars et al., 2015). The fault responsible for the earthquake is difficult to identify because it apparently did not rupture the surface. The main shock and many well-located aftershocks delineated a previously unrecognized southeast-dipping fault, since named the Quail fault (e.g., Horton and Williams, 2012; Horton et al., 2012). The modern seismogenic surface coincides with a zone of Paleozoic ductile strain related to the Long Branch fault, which may have guided brittle rupture in 2011 (Hughes et al., 2015). The Long Branch fault and the Spotsylvania fault zone are members of the northeast-trending Piedmont fault system and likely connect with the Stafford fault system near Fredericksburg (Powars et al., 2015). The northeast-trending Stafford fault system has been mapped from Fredericksburg to Washington, D.C.

The Stafford fault system displaces Paleozoic crystalline rocks and overlying Cretaceous to Pliocene-Pleistocene coastal plain formations (e.g., Mixon and Newell, 1977; Powars and

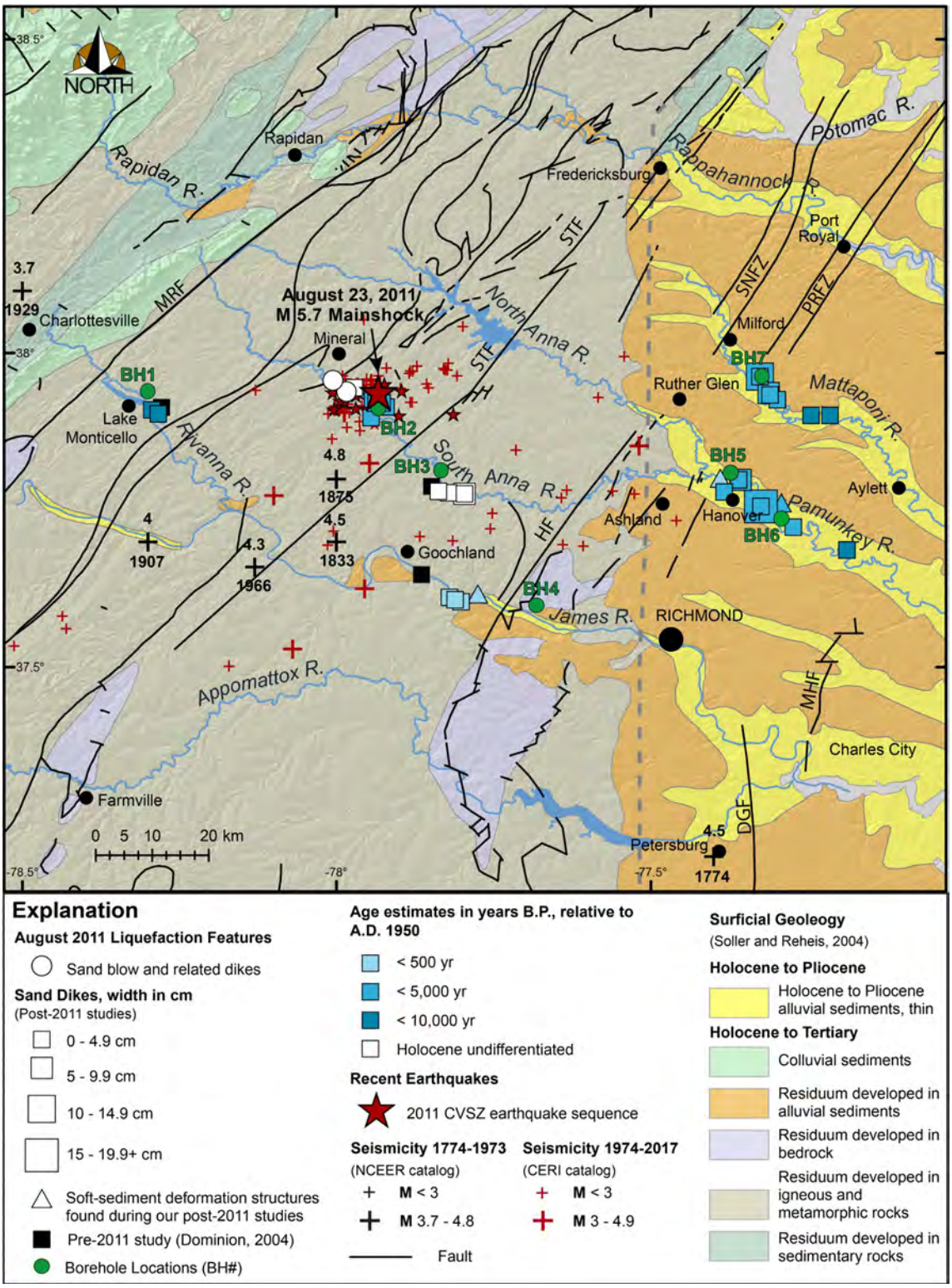

Figure 1. Map showing 2011 Virginia earthquake sequence (red stars), sand blows that formed in 2011 epicentral area (white circles), liquefaction features found during this and other post-2011 studies (blue and white squares & triangles) and during a pre-2011 study (black squares). Note locations of boreholes (green circles): data was used in the evaluation of scenario earthquakes. Fault zones: MRF=Mountain Run; STF= Stafford; HF=Hylas; SNFZ=Skinkers Neck; PRFZ= Port Royal; MF=Malvern Hill.

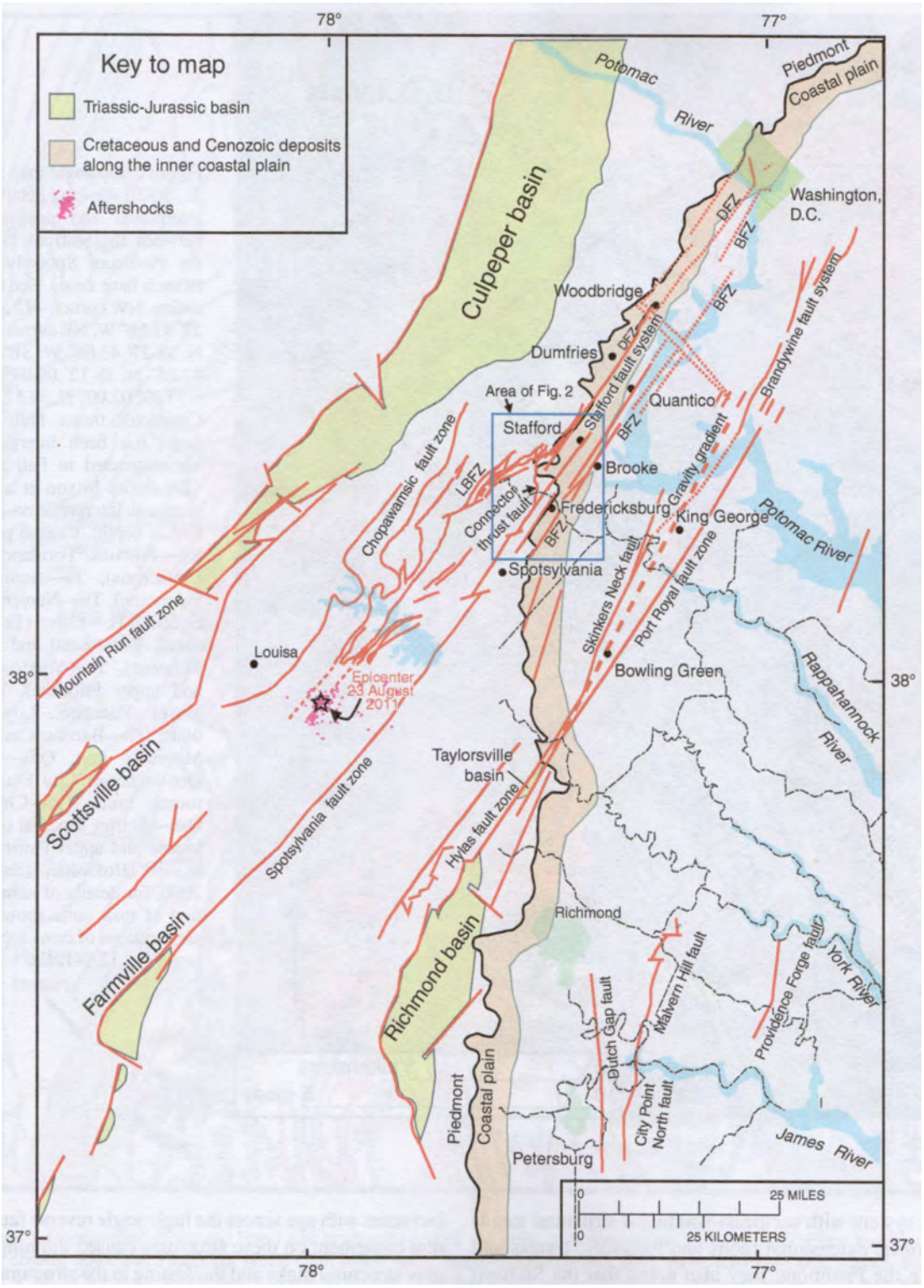

Figure 2. Map showing regional relations between Piedmont faults in vicinity of 23 August 2011 ***M*** *5.7 Mineral earthquake (star) and Stafford fault system to the northeast as well as other coastal faults to the east; LBFZ=Long Branch fault zone (from Powars et al., 2015).*

Horton, 2010; Powars et al., 2012; Figures 1 and 2). The Hylas fault zone is a zone of Paleozoic ductile shearing and thrusting along the western margins of the Richmond and Taylorville basins (e.g., Mixon et al., 2000). The faulted western edge of the Taylorville basin is closely aligned with the Skinkers Neck fault zone north of Richmond. The Skinkers Neck fault zone and other coastal plain fault zones including the Port Royal and Malvern fault zones are parallel to the Stafford fault system. The Skinkers Neck and Port Royal fault zones displace the middle Miocene Choptank Formation by about 4 m and the Malvern Hill fault zone east of Richmond displaces the early Pleistocene Bacon Castle Formation by more than 7 m (Powars et al., 2015). According to the authors, relatively high slip rates (4.4-27.4 m/m.y. compared to <1.0 m/m.y. for most of the past 110 m.y.) on these coastal faults during the Paleocene-early Eocene and Pliocene suggest episodic slip perhaps producing earthquakes. Further, they suggest that the Piedmont-Stafford fault systems may have produced earthquakes significantly larger than the Mineral earthquake if the combined length of the linked faults ruptured in a single event.

The 2011 **M** 5.7 mainshock is the largest earthquake to have occurred in the CVSZ during the historical period and has raised concerns about the earthquake potential of the seismic zone located only 130 km from the nation's capital. As suggested for other seismically active areas along the Atlantic passive margin, the CVSZ may represent a prolonged aftershock sequence of a large prehistoric earthquake (Ebel et al., 2000; Wolin et al., 2012). If so, the earthquake potential of the seismic zone might be greater than suggested by historical seismicity. Like the 1988 **M** 5.9 Saguenay, Quebec, event, the 2011 **M** 5.7 Virginia earthquake was not associated with surface rupture but induced liquefaction in its meizoseismal area (Tuttle et al., 1990; Green et al., 2015). Paleoearthquakes similar to these events would be missed by using the fault-trenching approach in paleoseismology, but could be recognized in the geologic record by using the paleoliquefaction approach (e.g., Obermeier, 1996; Tuttle, 2001; Green et al., 2005; Olson et al., 2005; Tuttle et al., 2019). Paleoliquefaction studies have helped to assess the earthquake potential of other seismic zones in the Central and Eastern North America (Tuttle and Hartleb, 2012). Paleoliquefaction studies both before and after the 2011 **M** 5.7 Mineral earthquake indicate that there is a record of past earthquakes in the CVSZ. This study aims to build on the finding of previous studies by conducting additional river surveys for paleoliquefaction features, dating additional paleoliquefaction features, and evaluating scenario earthquakes in order to improve estimates of the timing, location, and magnitude of earthquakes in the CVSZ during the Holocene.

Previous Liquefaction Studies in the Central Virginia Seismic Zone

During a paleoliquefaction study conducted in the mid-1990s, several weathered sand dikes (1 to 10 cm wide) were found at one site each on the James, Rivanna, and South Anna Rivers (Obermeier and McNulty, 1998; Dominion, 2004; Schindler et al., 2012). The paleoliquefaction features were attributed to at least one, and possibly three, moderate earthquakes during the Holocene. The apparent lack of widespread liquefaction features was interpreted as evidence that an earthquake of **M** > 7 had not occurred in the CVSZ during the past 10,000 years, though an earthquake in the **M** 6 to 7 range was not ruled out (Obermeier and McNulty, 1998; Dominion, 2004).

During a post-event survey of the 2011 Mineral earthquake, four small sand blows were found in and adjacent to the South Anna River near Yancy Mill, indicating that the moderate earthquake induced liquefaction in the epicentral area (e.g., Green et al., 2015). Subsequently, reconnaissance was performed in the fall of 2011 and after several storms, including Hurricane Irene. No 2011 liquefaction features were found on floodplains of the South Anna River in the Yancy Mill area or in cutbank exposures downstream from there for a distance of 24 kilometers (Tuttle and Busch, 2011). However, paleoliquefaction features, mostly bioturbated and weathered sand dikes, ranging in width from 1-5 cm, were found at eight sites along the South Anna River (Figure 1). Given that no 2011 liquefaction features were found along the South Anna River and that the paleoliquefaction features appeared to be getting larger in size towards the east, it was suggested that the paleoearthquake(s) responsible for the features may have been larger, and/or located farther to the east, than the 2011 event (Tuttle and Busch, 2011).

A NEHRP-funded paleoliquefaction study followed in 2015 and involved systematic surveys of cutbank exposures along the South Anna River to further study the paleoliquefaction there and along the Mattaponi, North Anna, and Pamunkey Rivers east of the Fall Line where liquefiable sediments are more common than in the epicentral area of the 2011 earthquake (Figure 1; Tuttle et al., 2015; Tuttle, 2016). In addition, surveys were conducted along the James and Rivanna (and tributary Stigger Creek) Rivers, where sand dikes were found during an earlier paleoliquefaction study in the 1990s (Obermeier and McNulty, 1998; Dominion, 2004). Paleoliquefaction features were confirmed along the South Anna River and Stigger Creek and fifteen additional liquefaction features, including sand dikes, sills, and soft-sediment deformation structures, were found along the James, Mattaponi, and Pamunkey Rivers (Figure 1). Similar paleoliquefaction features were also found along the South Anna River at the Horseshoe site upriver from Yancy Mill (Carter, 2015).

At least two episodes of earthquake-induced liquefaction were inferred on the basis of weathering characteristics of the liquefaction features, as well as dating of sediments in which liquefaction features formed. A few, slightly weathered, small ($\leq$ 3 cm) sand dikes and strata-bound soft-sediment deformation structures at three sites on the James and Pamunkey Rivers were thought to have formed during an earthquake in the past 500 years. The three sites occur in the southeastern part of the study area (near Richmond) suggesting that the earthquake may have been located in this area. More weathered and bioturbated sand dikes ($\leq$ 7 cm) and sills at sites on the Mattaponi, Pamunkey, and South Anna Rivers, as well as Stigger Creek, were thought to be more than 500 years old and to have formed in the past 4,500 years. Given the size and distribution of the liquefaction features across a 3,200 km^2 area (radius of ~45 km), it was hypothesized that the Late Holocene event may have been located farther to the east than the 2011 Mineral earthquake and to have been of $\mathbf{M} \geq 6$ (Castilla and Audemard, 2007).

Reconnaissance for Earthquake-Induced Liquefaction Features

River surveys for earthquake-induced liquefaction features originally were scheduled in late summer-early fall of 2018. However, frequent heavy rainfalls, some related to Hurricanes Florence, Gordon, and Michael, led to repeated flooding of rivers in central Virginia, prohibiting the surveys during that time period. Therefore, river surveys were postponed until late summer-early fall of 2019. River levels were very low at that time which afforded good exposure of

cutbanks. In addition, flooding during the previous year had scoured cutbanks and caused slumping of banks which contributed to exposure. Due to an abundance of downed trees and low water conditions, however, there were many log jams in the Mattaponi and Pamunkey Rivers that impeded and slowed our surveys. Nevertheless, we surveyed 30 km of the Mattaponi River and 39 km of the Pamunkey River, as well as 8 km of the James River, for a total of 77 km. Study sites where we collected detailed information are described below and summarized in Table 1.

James River

Along the James River, we searched cutbanks for liquefaction features for 8 km between Powhatan State Park and the Rt. 522 bridge at Goochland west of Richmond (Figure 1). In this area, the river is flanked mostly by Holocene fluvial terraces. Cutbanks in the terraces ranged from 0.5 to 4.5 m in height. Exposure was fairly limited and included a few slump scarps and the lower 0.5 to 1.5 m of cutbanks that were eroded by wave action. Exposures revealed mostly mottled silt underlain by clayey silt. The upper portions of the cutbanks were usually covered by tree roots, grass, and shrubs.

At site JR200 and other nearby exposures, where sand was interbedded with silt, small soft-sediment deformation structures, including sand diapirs (~1 cm wide) had formed (Table 1). A sample of leaves (JR200-L1), collected from silt about 30 cm above the water level and 15 cm below soft-sediment deformation structures, yielded a 2-sigma calibrated radiocarbon age of Post 1950 (Table 2), indicating that the sediment and deformation structures are modern.

If the small sand diapirs were related to earthquake-induced liquefaction, the 2011 **M** 5.7 earthquake would be the most likely triggering event. However, river levels in the region were very low at the time of the 2011 Virginia earthquake. According to USGS surface-water daily statistics (http://waterdata.usgs.gov/nwis/dvstat?referred_module=sw) for monitoring stations on the James River, river discharge was so low on August 23, 2011 that the sandy layer in which the deformation structures occur would not have been saturated, and therefore, could not have liquefied. Therefore, it seems more likely that these small features formed as the result of non-seismic sedimentary processes such as rapid sedimentation.

Mattaponi River

We searched 30 km of the Mattaponi River along two sections, including 5 km downstream from the Rt. 2 bridge and 25 km upstream from the Rt. 628 bridge (Figure 1). Along both portions of the river, Holocene fluvial deposits are inset into Quaternary and Tertiary deposits (Mixon et al., 1989). Along the upper portion, cutbanks in Holocene deposits range from 2-3 m in height and exposure is generally fair, except in river bends where it is good. Most of the cutbanks reveal mottled and bioturbated sandy silt. In some places, fine-medium sand occurs below the sandy silt. In other places, sand was found from 5 to 60 cm below the water level (BWL) using a soil probe. Along the lower portion of the river, cutbank height, quality of exposure, and stratigraphy is similar to the upper portion of the river. The sedimentary conditions along both portions of the river are conducive to the formation of liquefaction features. The main difference between the

two portions of the river is that the Holocene floodplain is broader along the lower portion, suggesting that a wider age range of deposits may be exposed in the cutbanks.

Table 1. Study sites in the CSVZ region.

Site	Longitude °W	Latitude °N	Cutbank Exposure	Exposed Sediment[1]	Liquefaction Feature[1]	Weathering of Feature
James River						
JR200	77.74142	37.68256	Cutbank: 4.5 m high; only lower 0.5 m well exposed	Interbedded, silt & cross-bedded sand	Small sand diapirs	Iron stained
Mattaponi River						
MR100	77.24297	37.90092	Cutbank: 2.5 m high; good exposure	Silty sand and pebbly fine-medium sand underlain by mottled silt & dark gray silt followed by pebbly sand	Two sand dikes – 4 cm & 3.5 cm wide; coarse-fine sand with few pebbles & silt clasts; extend to 0.45 m AWL or 2.05 m BS.	Iron stained
MR101	77.21323	37.90080	Cutbank: 2 m high; lower 1 m well exposed	Mottled silt	Two sand dikes – 0.5 cm & 0.2 cm; pinch out 1 m & 0.5 m AWL or 1 m & 1.5 m BS	None observed
MR102	77.33176	37.96163	Cutbank: 3 m high; good exposure	Mottled sandy silt underlain by fine-medium sand	None observed; organic samples collected for dating	Not applicable
MR103	77.32673	37.96193	Cutbank: 2.5 m high; good exposure	Mottled sandy silt; probe – silty fine sand to coarse sand from 3-26 cm BWL	Sand dike – 14 cm wide; branches upward, forming two 1-cm-wide dikes; medium-fine sand; extend to 0.8 m AWL	Upper portion of dikes bioturbated
MR104	77.17000	37.89487	Cutbank: 1.75 m high; good exposure	Mottled sandy silt underlain by medium-coarse sand	None observed; organic samples collected for dating	Not applicable
Pamunkey River						
PR100	77.27311	37.72181	Cutbank: 4 m high; good exposure	Mottled silt	Two sand dikes – 4 cm & 0.5 cm wide; silty fine sand; extend to at least 0.67 m AWL	Upper portion of dikes bioturbated

[1] Abbreviations: AWL = above water level; BWL = below water level; BS = below surface.

Table 1 Continued. Study sites in the CSVZ region.

Site	Longitude °W	Latitude °N	Cutbank Exposure	Exposed Sediment[1]	Liquefaction Feature[1]	Weathering of Feature
Pamunkey River						
PR101	77.32460	37.75471	Cutbank: 3 m high; good exposure	Mottled and bioturbated silt and silty sand underlain by cross-bedded medium sand	Sand dike – 20 cm wide; coarse-medium sand with flow structure & clasts; pinch out 1.25 m AWL or 1.75 m BS; also, sand diapirs, foundered clasts, & disturbed bedding	Upper portion of diapirs & dike biotur-bated and mottled
PR102	77.32120	37.73563	Cutbank: 3 m high	Mottled silt underlain by interbedded silty sand & medium-coarse sand followed by pebbly sand.	None observed	Not applicable
PR103	77.30836	37.73566	Cutbank: 3 m high; good exposure	Mottled silt, some layering, underlain by interbedded sand & clay; probe – sand to 85 cm BWL	None observed, good conditions for formation	Not applicable
PR105	77.21173	37.68204	Cutbank: 1.5 m high; fair exposure	Mottled clay silt	None observed, organic samples collected for dating	Not applicable
PR106	77.18650	37.68618	Cutbank: 1.75 m high; lower 1 m good exposure; upper section very vegetated	Mottled and bioturbated silt grades to silty clay; probe – silty clay to 0.1 m BWL	Three, silty very fine sand dikes; 5 cm, 2 cm, & 0.4 cm wide; largest dikes pinches out 0.45 m AWL	Bioturbated

[1] Abbreviations: AWL = above water level; BWL = below water level; BS = below surface.

Table 2. Radiocarbon dating of organic samples in the CVSZ.

River Site-Sample# Lab-#	$^{13}C/^{12}C$ Ratio	Conventional Radiocarbon Age Yr B.P.[1]	Calibrated Radiocarbon Age Yr B.P.[2]	Calibrated Calendar Date A.D./B.C.[2]	Sample Description[3]
James River					
JR200-L1 Beta-546849	-23.4	106.03 ± 0.4 pMC	Post 1950	AD 2009-2004 AD 1957-1956	Plant material; collected from leaf litter in silt ~30 cm AWL and 15 cm below soft-sediment deformation structures
Mattaponi River					
MR102-C1 Beta-546852	-25.6	2490 ± 30	2459-2730	510-781 BC	Charred material; large angular chunk collected from sand ~50 cm AWL & 66 cm below silt/sand contact; sand possible source of dikes at nearby sites
MR104-C1 Beta-547638	-24.8	6140 ± 30	6951-7158	5002-5209 BC	Charred material; small angular piece collected from sand ~55 cm AWL or 15 cm below mottled sandy silt/sand contact; sand possible source of dikes along lower river
Pamunkey River					
PR101-C1 Beta-547635	-27.1	2860 ± 30	2878-3067	929-1118 BC	Charred material; small angular piece collected ~75 cm AWL or 225 cm BS from mottled sandy silt and mottled silt intruded by diapirs and dike
PR103-L1 Beta-546850	-29.6	120 ± 30	10-150 186-272	AD 1940-1800 AD 1764-1678	Plant material; horizontally bedded leaf litter collected ~25 cm AWL from thin clay layer
PR105-L1 Beta-546851	-25.7	122.96 ± 0.46 pMC	Post 1950	AD 1983-1981 AD 1961-1958	Plant material; horizontally bedded leaves collected ~70 cm BWL from thin sand within silty clay
PR106-C1 Beta-547636	-25.7	5990 ± 30	6741-6907	BC 4958-4792	Charred material; small angular piece collected 23 cm AWL or 152 cm BS from mottled silt intruded by dikes

[1] Conventional radiocarbon ages in years B.P. or before present (1950) determined by Beta Analytic, Inc. Errors represent 1 standard deviation statistics or 68% probability.

[2] Calibrated age ranges as determined by Beta Analytic, Inc., using the Pretoria procedure (Talma and Vogel, 1993; Vogel et al., 1993). Ranges represent 2 standard deviation statistics or 95% probability.

[3] Abbreviations: AWL = above water level; BWL = below water level; BS = below surface.

Along the upper portion of the river, liquefaction features occur at site MR103 located about 2 km downstream form the Rt. 2 bridge. At the site, the cutbank is 2.5 m high and exposes mottled and bioturbated sandy silt (Table 1). Probing below the cutbank, silty fine sand grades to coarse sand from 3-26 cm BWL. A 14-cm-wide dike of silty, medium-fine sand is exposed at the base of the cutbank (Figure 3). The dike branches upward to form two, 1-cm-wide dikes. One of the dikes pinches out quickly but the other dike extends higher in the cutbank. It was crosscut by a root cast; however, we removed the root mold and found that the sand dike continues upsection to 0.8 m above the water level (AWL), or 1.7 m below the surface (BS) of the floodplain. The upper 1.7 m of the cutbank is very bioturbated. The dike may have extended higher in the section and been destroyed by bioturbation. No organic sample was found at this site for radiocarbon dating. However, at site MR102 located about 0.5 km upstream, we collected a large angular piece of charred material from fine-medium sand 66 cm below the contact with mottled sandy silt above. The sample yielded a 2-sigma calibrated age of 2459-2730 yr B.P. (before A.D. 1950) (Table 2). This age likely reflects that of the sand deposit that occurs below mottled sandy silt at both MR102 and MR103. If so, it provides a maximum constraining age of 2730 yr B.P. for the sand dikes at MR103. The sand deposit may be the source of the sand dikes at MR103.

Along the lower portion of the river, liquefaction features occur at sites MR100 and MR101, located 19 and 14 km upstream from the Rt. 628 bridge, respectively. At MR100, the cutbank is 2.5 m high and exposes silty sand and pebbly fine-medium sand underlain by mottled and bioturbated silt and dark gray silt followed by pebbly sand. Three dikes originating in the pebbly sand at the base of the cutbank intrude the overlying dark gray silt. Two of the dikes, ranging up to 4 cm wide, pinch out in the dark gray silt. The third dike, 3.5 cm wide, extends into the mottled silt above to 0.45 m AWL or 2.05 m BS. The dikes are composed of coarse-fine sand, contain a few small pebbles and silt clasts, and are iron stained.

At MR101, the cutbank is only 2 m high and exposes mottled silt. At nearby sites both upstream and downstream from MR101, sand below the mottled silt is exposed in the lower part of the cutbank. At MR101, two sand dikes, 0.5 cm and 0.2 cm wide, intrude the mottled silt and pinch out 1 m and 0.5 m AWL, respectively.

No organic sample was found at either MR100 or MR101 for radiocarbon dating. However, at MR104, we collected a small angular piece of charred material from the sand deposit 15 cm below the contact with mottled silt. The sample yielded a 2-sigma calibrated age of 6951-7158 yr B.P. (before A.D. 1950) (Table 2) and likely reflects the age of the sand deposit below mottled silt along the lower portion of the river. Therefore, the sample provides a maximum constraining age of 7160 yr B.P. for the sand dikes at MR100 and MR101.

The sand dikes site at MR100, MR101, and MR103 along the Mattaponi River are interpreted to be earthquake-induced liquefaction features. The dikes appear to originate in a sandy deposit, intrude an overlying silt deposit, are composed of coarse-fine sand, and branch or pinch upward. At all three sites, the host sediment is mottled and bioturbated. The sand dikes are more obvious deeper in the section and become more bioturbated, weathered, and difficult to trace higher in the section.

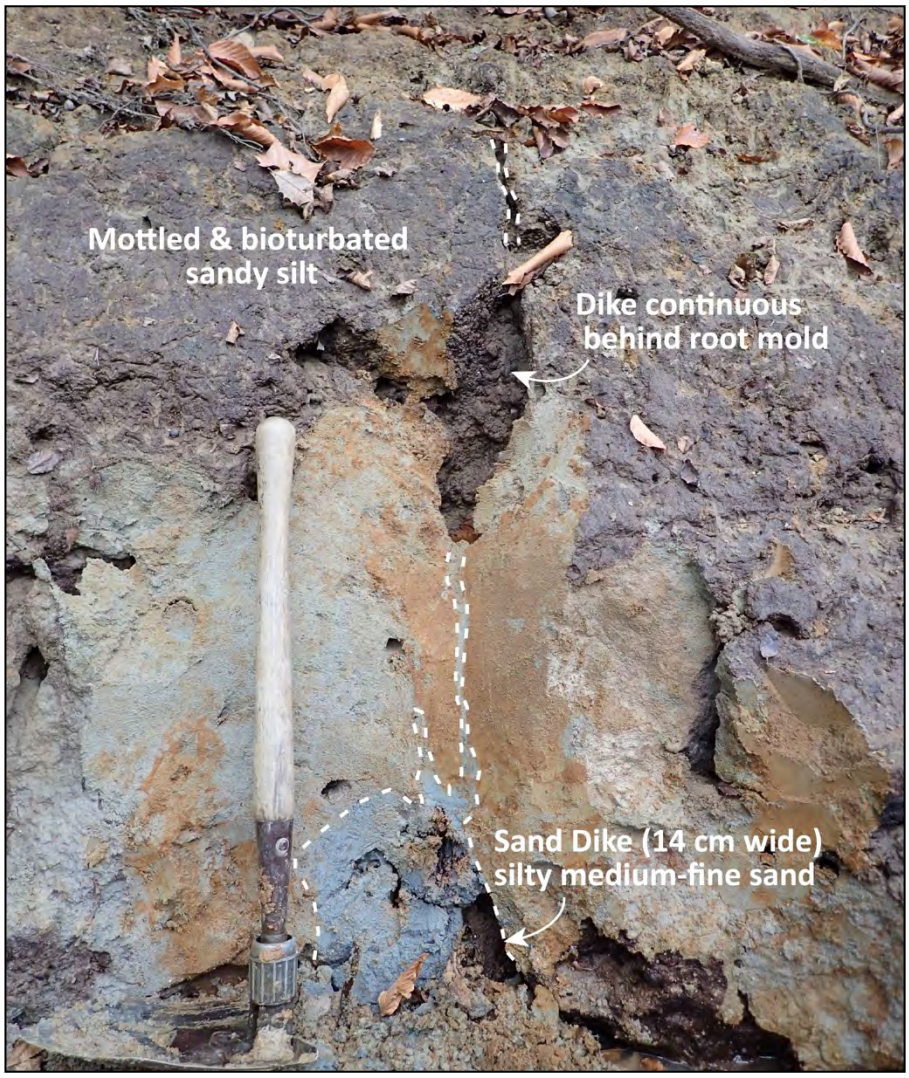

Figure 3. Photograph of sand dikes at site MR103. A 14-cm wide sand dike, branches upward to form two, 1-cm wide dikes. One of the dikes continues upsection, is disturbed by root mold, and extends to 0.8 m AWL. Above that, the dike may have been destroyed by bioturbation. For scale, shovel handle is 50 cm long.

Some of the dikes are also disturbed by bioturbation. The degree of bioturbation and weathering of the host sediment and the sand dikes suggest that they are paleoin age. Radiocarbon dating suggests that the apparently ubiquitous sand, and the likely source of the dikes, was deposited from 7160 to 2730 yr B.P. Dating of the sand deposit provides maximum constraining ages of 7160 yr B.P. for dikes at MR100 and MR101 and of 2730 yr B.P. for dikes at MR103. These do not represent close maximum ages, and currently there are no minimum constraining ages for any of the sand dikes. Also, there are no crosscutting relationships of liquefaction features to indicate multiple liquefaction events. Therefore, there is uncertainty about the number and timing of earthquakes that induced liquefaction along the Mattaponi River. We are confident that there was at least one paleoearthquake large enough to induce liquefaction along the river during the past 7210 years.

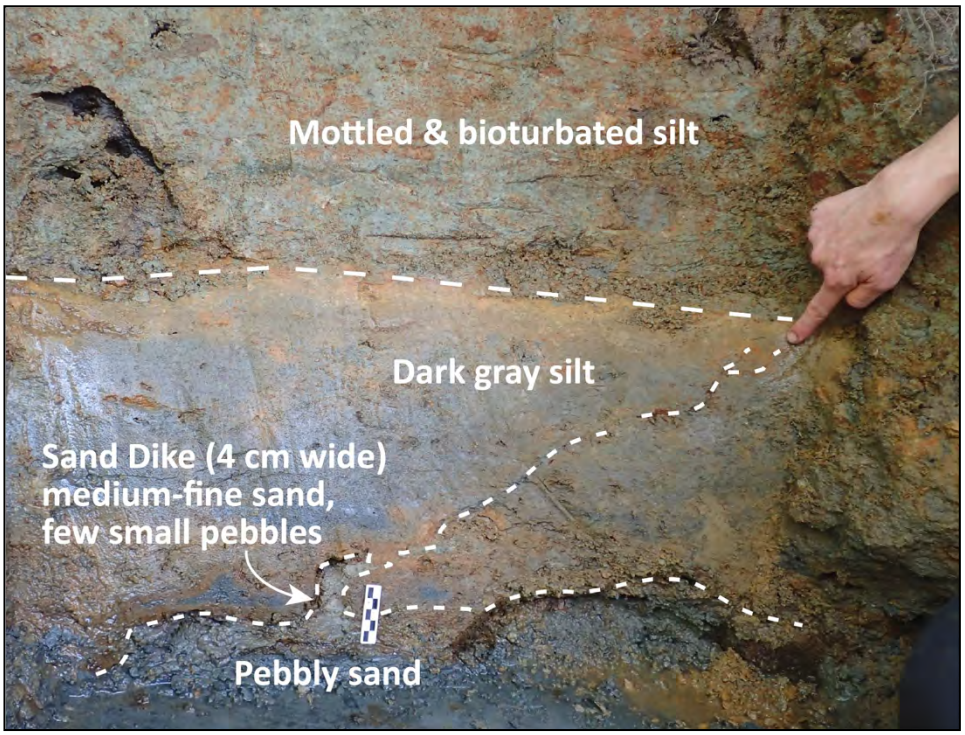

Figure 4. Photograph of 4 cm wide sand dike at site MR100. Dike originates in pebbly sand at the base of the cutbank, intrudes overlying dark gray silt, and pinches out 35 cm AWL. Black and white intervals on scale represent centimeters.

Pamunkey River

We searched 39 km of the Pamunkey River from the Hanover Juvenile Correctional Facility downstream to 0.5 km past the Rt. 360 bridge (Figure 1). Along this portion of the river, the Holocene-Pleistocene floodplain is fairly wide and is under cultivation. Holocene fluvial deposits are inset into Quaternary and Tertiary deposits (Mixon et al., 1989). At least three terrace levels – 4 m, 8 m, and 15 m+ – along the river were noted. The low terrace is Holocene in age; the middle terrace is likely Pleistocene in age; and the high terrace is probably Tertiary in age.

Exposure along the river was generally fair and better in river bends. There are many exposures of Holocene deposits and only a few exposures of Pleistocene deposits. Cutbanks in Holocene deposits range from 1.5-4 m in height and expose mottled silt, mottled silt underlain by clayey silt, mottled silt interbedded with sand, mottled silty sand, and mottled silt underlain by sand and pebbly sand. If it was not exposed at the base of the cutbanks, sand was often encountered with a soil probe within 0.4-0.8 m BWL. These sedimentary conditions are conducive to the formation of liquefaction features. Cutbanks in Pleistocene deposits are about 6-8 m in height and expose pebbly sand underlain by silt or clay. These sedimentary conditions are not conducive to the formation of liquefaction features. Along the lower 8 km of the portion of the river searched, cutbanks in Holocene and Pleistocene deposits were only 1.5-2.5 m and 6-8 m in height, respectively. This decrease in cutbank exposure was due to a rising tide at the time of the survey. In several places, the meandering river has reached the edges of the Holocene floodplain creating high (15-30 m) cutbanks in Tertiary deposits.

Site PR101 is located about 1 km downriver from the correctional facility. At the site, the cutbank is 3 m high and exposes mottled and bioturbated silt and silty sand underlain by iron-stained crossbedded medium sand (Figure 5). Sand diapirs of the medium sand appear to intrude the overlying mottled silt and sandy silt and clasts of the overlying material appear to have foundered into the medium sand. The sand deposit is crosscut by a sand dike characterized by coarse-medium sand, flow structure, and clasts. Also, the bedding of the sand deposit is disturbed adjacent to the dike and below the sand diapirs. The upper portions of the diapirs and dike are bioturbated and mottled, suggesting they are prehistoric in age. We collected a small angular piece of charred material, PR101-C1, from the mottled silty sand intruded by the sand diapirs and sand dike. The sample yielded a 2-sigma calibrated age of 2878-3067 yr B.P. (Table 2). This age likely reflects that of the basal portion of the silty sand deposit and provides a maximum constraining age of 3070 yr B.P. for the diapirs and dike at this site.

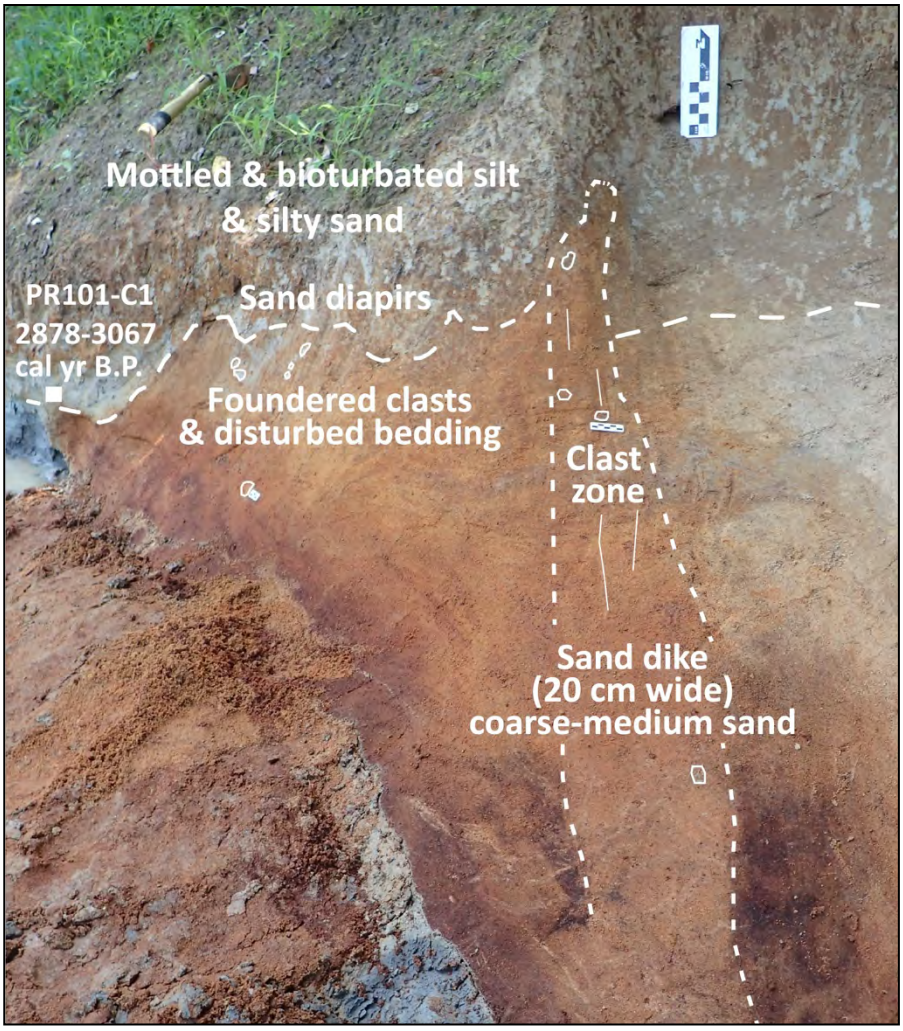

Figure 5. Liquefaction features at site PR101 include a 20 cm wide sand dike, characterized by flow structure and clasts, as well as sand diapirs intruding overlying mottled silt and silty sand. Clasts of overlying silty sand appear to have foundered into the underlying sand layer. On the scale near top of photograph, black and white intervals represent decimeters (upper) and centimeters (lower).

Site PR100 is located about 2 km downriver from the Rt. 605 bridge. Here, the cutbank is 4 m high and exposes mottled silt. Two sand dikes, 4 cm and 0.5 cm wide and composed of silty fine sand, intrude the mottled silt, and pinch out about 0.67 m AWL. Sandy domains above the dikes are probably bioturbated upper portions of the dikes. No organic sample was found at this site. However, sample PR101-C1 from the silty sand below mottled silt at site PR101 provides a maximum constraining age of 3070 yr B.P. for the mottled silt along this part of the river, and therefore, the sand dikes that intrude mottled silt at PR100.

Site PR106 is located about 1 km upstream from the Rt. 360 bridge. At the site, the cutbank is only 1.75 m high. The upper part of the cutbank is very vegetated but the lower 1 m is well exposed. It reveals mottled and bioturbated silt which grades to a clayey silt at about water level. The clayey silt continued below the water level but was difficult to penetrate with the soil probe. Three dikes, 5 cm, 2 cm, and 0.4 cm wide and composed of silty, very fine sand, are exposed along a 6-m long zone at the base of the cutbank. The two smaller dikes pinch out within 0.3 m AWL. The largest dike branches upward to form several smaller dikes that pinch out within 0.45 m AWL (Figure 6). The upper portions of the dikes appear bioturbed, suggesting that they are prehistoric in age. We collected a small angular piece of charred material, PR106-C1, from the mottled silt intruded by sand dikes. The sample yielded a 2-sigma calibrated age of 6741-6907 yr B.P. (Table 2). This age likely reflects that of the silt deposit and provides a maximum constraining age of 6910 yr B.P. for the dikes at this site.

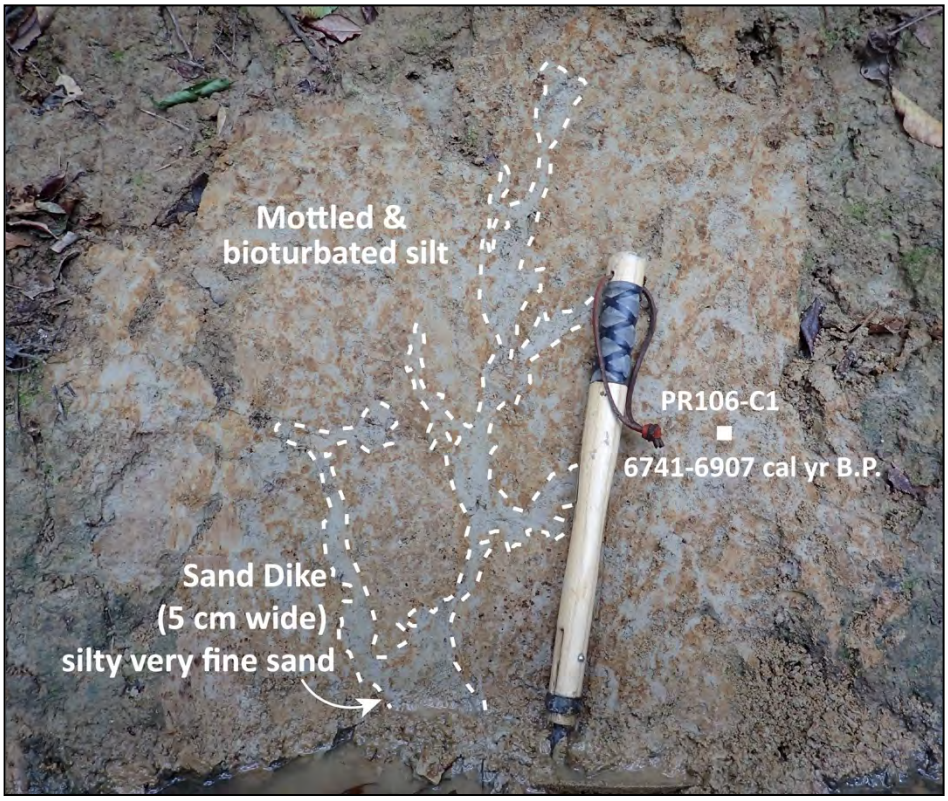

Figure 6. Photograph of 5-cm-wide sand dike at site PR106. Dike is composed of gray silty, very fine sand, branches and extends upsection, and crosscuts mottled silt. Dating of charred material from the mottled silt provides maximum constraining age and indicates that the dikes formed since 6910 yr B.P. For scale, scarper handle is 36 cm long.

Along the Pamunkey, the sand dike and sand diapirs at PR101 as well as sand dikes at PR100 and PR106 are interpreted to be earthquake-induced liquefaction features. The dike and diapirs at PR101 originate in a coarse-medium sand deposit, in which bedding has been disturbed by liquefaction and fluidization, and intrude the base of the overlying mottled sandy silt and mottled silt deposits. The dikes at PR100 and PR106 composed of silty fine-very fine sand intrude mottled silt in which they terminate. At all three sites, the host sediment is mottled and bioturbated. The sand dikes and diapirs are either bioturbated or mottled, suggesting that they are prehistoric in age. Radiocarbon dating below mottled silt at PR101 suggests that the liquefaction features that formed at this site as well as PR100 formed since 3070 yr B.P. Dating of mottled silt at PR106 farther downriver provides a maximum constraining age of 6910 yr B.P. for dikes at the site. Like the sand dikes on the Mattaponi River, there are no close maximum or minimum constraining ages nor are there crosscutting relationships for any of the sand dikes. As a consequence, there is uncertainty about the number and timing of earthquakes that induced liquefaction along the Pamunkey River. However, there clearly was at least one paleoearthquake large enough to induce liquefaction along the river during the past 6910 years.

Interpretation of Timing, Locations, and Magnitudes of Earthquakes

Based on findings during this study and our previous NEHRP-funded study in 2015, there are at least two generations of liquefaction features that formed in the CVSZ prior to the 2011 Mineral earthquake. The younger generation of features exhibits relatively little iron staining or mottling and formed in sediment that was deposited since 280 and 430 yr B.P. They are small (dikes ≤ 3 cm wide) and few in number, and are narrowly distributed on the James and Pamunkey Rivers (Figure 1 and Table 3). In comparison, the older generation of features exhibits bioturbation and mottling and formed in sediment ranging in age from 2730 to 9460 yr B.P. They are larger (dikes up to 20 cm wide), more numerous, and more broadly distributed on the Mattaponi, Pamunkey, South Ann, and Rivanna Rivers than the younger generation (Figure 1 and Table 3).

Table 3. Earthquake-induced liquefaction features in the study region.

River	Features	Maximum Dike Width (cm)	Weathering	Maximum Age Constraint Yr B.P. (1950)	Event
Mattaponi	Sand dikes	14	Bioturbation & mottling	2730 & 7160	Late Holocene
James	Sand dikes & SSDs	3	Some mottling	280	1875
Pamunkey	Sand dikes and SSDs	20	Bioturbation & mottling	430, 3070 & 6910	1875 Late Holocene
South Anna	Sand dikes	5.5	Bioturbation & mottling	4440	Late Holocene
Rivanna	Sand dikes	2.7	Bioturbation & mottling	9460	Late Holocene

In all cases, age control on the formation of the liquefaction features is based on dating of sediment below or in which the features formed. Therefore, dating provides maximum

constraining ages, and not necessarily close maximum constraining ages, of the liquefaction features. Unfortunately, we have no minimum constraining ages to help bracket and narrow age estimates of the features. Within each generations of liquefaction features, there are no substantial weathering differences to suggest that they formed during multiple earthquakes separated in time. In addition, there are no crosscutting relationships of liquefaction features to indicate multiple earthquakes. Neither weathering characteristics nor lack of crosscutting relationships are criteria by which to rule out multiple events, but there is no evidence to support multiple events during either the historic or prehistoric periods in question. If we assume that all the features in each generation formed during one event and that the youngest maximum constraining age for each generation most closely approximates a close maximum constraining age, the younger generation of features formed since 280 yr B.P. or during the past 350 years; and the older generation of features likely formed before 280 yr B.P. and since 2730 yr B.P. or between 350-2800 years ago (Figure 7).

The 1875 **M** 4.8 ± 0.2 earthquake is the largest historical event to strike this area during the past 350 years. The earthquake was assigned a maximum modified Mercalli intensity (MMI) of VII based on accounts of earthquake effects (Eppley, 1965). An MMI VI-VII area was drawn to include Richmond and nearby counties to the northwest and south (Hopper and Bollinger, 1971). Damage was concentrated in Richmond and along the James River (Oaks and Bollinger, 1986). Although poorly constrained, the earthquake's location is thought to be northwest of Goochland (Figure 7). Regardless of its exact location, the earthquake generated intensity VII shaking along the James River, which could have induced liquefaction in very susceptible sediment. Although we cannot be certain that it was responsible for the historic liquefaction features on the James and Pamunkey River, the 1875 earthquake seems like the most likely candidate.

According to the relation between earthquake magnitude and greatest distance to liquefaction effects (Castilla and Audemard, 2007), an earthquake of **M** ≥ 4.8 can induce liquefaction up to 15 km from its epicenter and an earthquake of **M** ≥ 5 can induce liquefaction up to 18 km from its epicenter (Figure 8). The distance between the assigned location for the earthquake northwest of Goochland and the liquefaction features on the James River is 28 km. According to the magnitude and distance relation, it takes a **M** ≥ 5.5 to induce liquefaction at that distance. This suggests that the earthquake was either more than a 0.5 magnitude greater than **M** 4.8 or located closer to the James River liquefaction sites. The distance between the historical liquefaction features on the James and Pamunkey Rivers is about 40 km. A **M** ≥ 5 earthquake located between the two rivers in the vicinity of a cluster of seismicity near Ashland might explain the distribution of the features especially since northeast-southwest oriented geologic structure and faults in the area could have guided ground motion towards the James and Pamunkey Rivers. Alternatively, perhaps the 1875 **M** 4.8 ± 0.2 earthquake occurred within 15 km of the James River sites and another small earthquake occurred in close proximity to the Pamunkey River site.

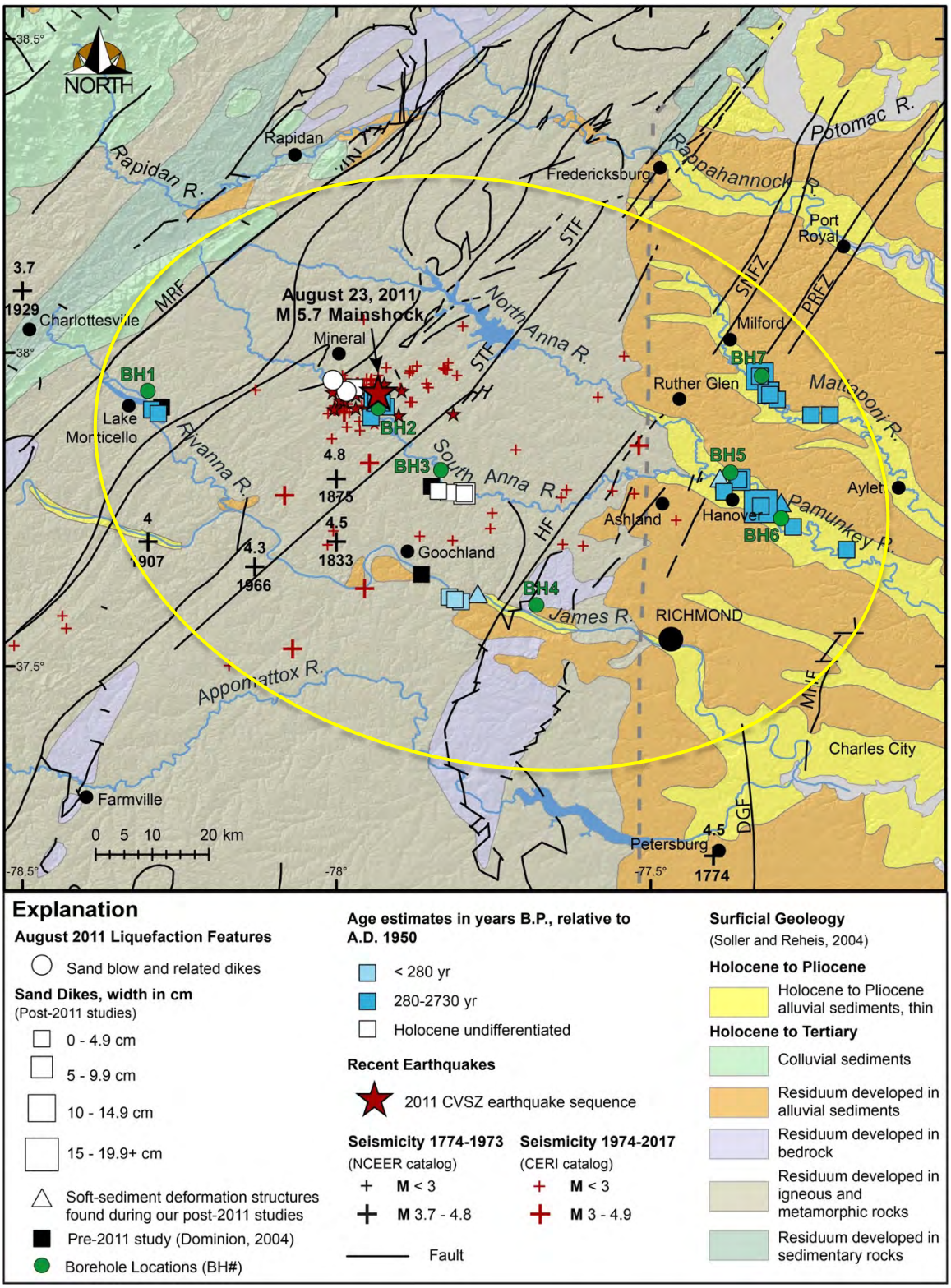

Figure 7. Map showing liquefaction features attributed to two earthquakes: an historic earthquake that occurred since 280 yr B.P., most likely the 1875 event, and a paleoearthquake that occurred between 280-2730 yr B.P. or 350-2800 years ago. Yellow ellipse delineates area within which liquefaction features have been found.

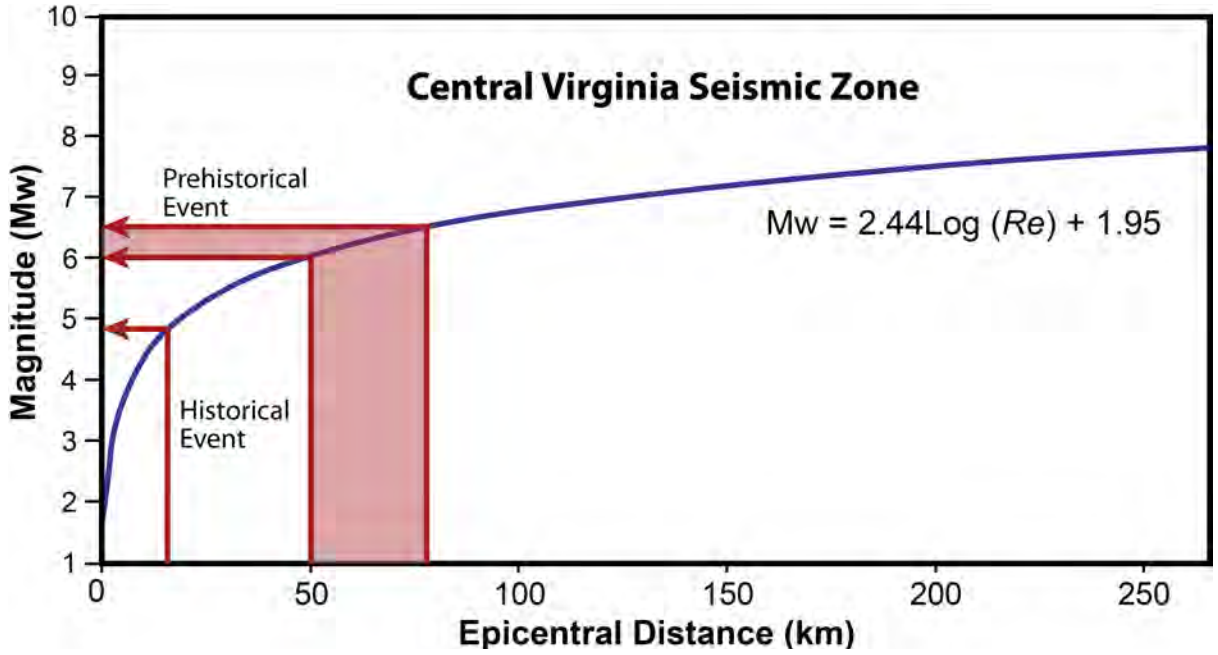

*Figure 8. Relation between moment magnitude (**M**w) and epicentral distance (Re) to farthest liquefaction effects in very susceptible sediment developed from worldwide data (modified from Castilla and Audemard, 2007). According to the relation, the 1875 **M** 4.8 earthquake could induce liquefaction along the James River if it were located within 15 km. If the 1875 event were **M** 5 and located between the James and Pamunkey Rivers, it could be responsible for historical features on both rivers. A **M** ≥ 6 paleoearthquake centered within the paleoliquefaction field could induce liquefaction along the Mattaponi, Pamunkey, South Anna, and Rivanna Rivers. A **M** ≥ 6.5 paleoearthquake centered near Ashland could explain the occurrence of larger liquefaction features along the Mattaponi and Pamunkey Rivers as well as the regional distribution of features.*

As mentioned above, the older generation of features likely formed between 350-2800 years ago (Figure 7) even though some of the maximum constraining ages date back to 9460 yr B.P. Formation of the features during the Late Holocene seems more likely given that sea level along Virginia's Eastern Shore was > 3 m lower than modern sea level prior to 2800 yr B.P. and > 5.5 m lower than modern sea level prior to 4000 yr B.P. (Figure 9; Van de Plassche, 1990). Sea level is the regional base level and influences coastal rivers, especially those in the tidal zone. Prior to 2800 yr B.P., a lower water table along the rivers in the CVSZ may have reduced the liquefaction susceptibility of Holocene sediment. Furthermore, if the water table was below the sandy source beds of the liquefaction features, the source beds could not have liquefied.

In addition to sea level, the water table is influenced by many local factors and fluctuates during the course of a year. Sediment was being deposited along the rivers area during the Early-Middle Holocene, and therefore, liquefaction events cannot be completely ruled out during this time period. However, a significantly lower sea level may have limited the time during which liquefaction could occur along the rivers. Therefore, liquefaction features are more likely to have formed during the Late Holocene, and there may be large gaps in the paleoliquefaction record during the Middle and Early Holocene.

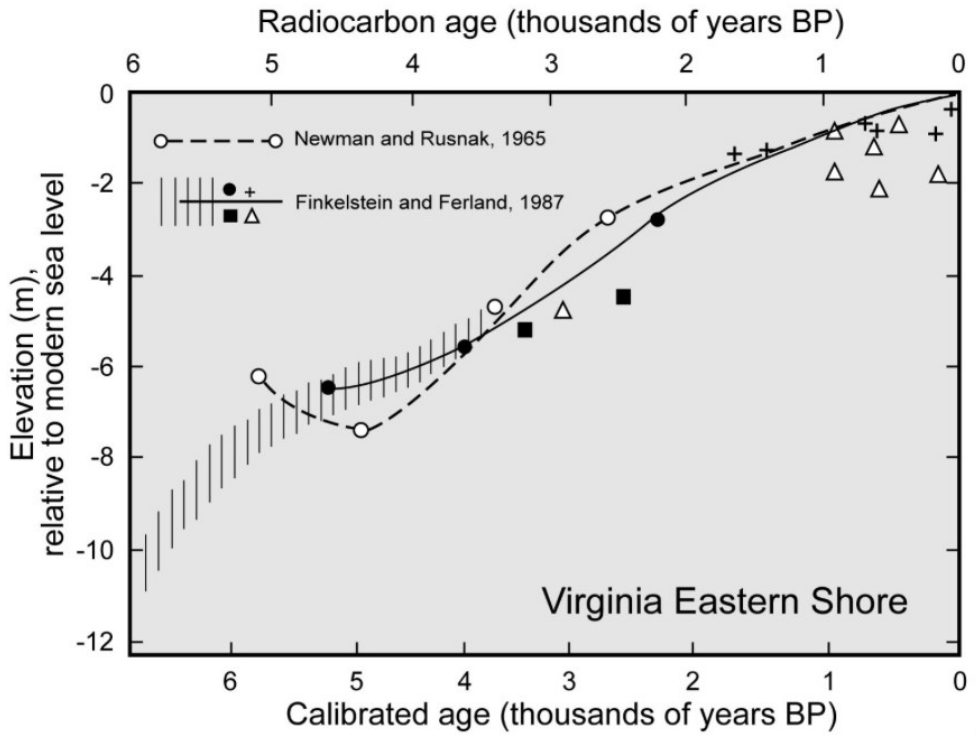

Figure 9. Middle to Late Holocene sea-level curve for Virginia Eastern Shore (from Van de Plassche, 1990).

As mentioned above, the paleoliquefaction features are larger, more numerous, and more broadly distributed than the historical features, and there is no evidence to indicate that they formed during more than one earthquake. According to the magnitude-distance relation (Castilla and Audemard, 2007), a **M** ≥ 6 paleoearthquake centered within the currently known paleoliquefaction field could have been responsible for liquefaction along the Mattaponi, Pamunkey, South Anna Rivers, and Rivanna Rivers (Figure 8). If the paleoearthquake were produced by the 2011 Mineral source, it would have to be of **M** ≥ 6.5 to induce liquefaction 75 km away at the most distant site on the Pamunkey River as well as along the other rivers.

The largest paleoliquefaction features occur on the Pamunkey and Mattaponi Rivers, suggesting that the source of the paleoearthquake that led to their formation may be nearby. A cluster of small earthquakes near Ashland indicates that there is an active fault in the area (Figure 7). Although several faults have been mapped in the area, they may or may not be the source of the earthquakes. If the paleoearthquake were located near Ashland, it would have to be of **M** ≥ 6.5 to induce liquefaction 75 km away at the most distant site on the Rivanna River, as well as along the other rivers.

We've considered several plausible locations and magnitudes of paleoearthquakes that could explain the distribution of paleoliquefaction features. Other combinations are also possible and the full extent of paleoliquefaction features is not yet known. Based on the currently available information, we favor a **M** ≥ 6.5 earthquake centered near Ashland because it better explains the size variation as well as the regional distribution of liquefaction features.

Evaluation of Scenario Earthquakes

In this study, scenario earthquakes are evaluated for a source similar to that which produced the 2011 Mineral, VA, earthquake and a source in the Ashland area where numerous small earthquakes have been recorded since 1974 and closer to the larger paleoliquefaction features along the Pamunkey and Mattaponi Rivers (Table 4; Figure 7). We determine whether or not various scenario earthquakes produced by these two possible sources could be responsible for the formations of liquefaction features along the James, Mattaponi, Pamunkey, South Anna, and Rivanna Rivers (Figure 7).

Table 4. Scenario earthquakes evaluated using liquefaction potential analysis.

Source	Magnitudes (M)	Distances (km)
Similar to 2011 Mineral earthquake	5.5, 5.75, 6.0, 6.25, 6.5, 6.75, 7.0	10, 20, 30, 45, 55, 58, 65
Ashland area	5.5, 5.75, 6.0, 6.25, 6.5, 6.75	10, 16, 18, 33, 35, 45, 78

Liquefaction Potential Analysis

The scenario earthquakes are evaluated using the cyclic stress method, also known as the simplified procedure, for assessing liquefaction potential (e.g., Seed and Idriss, 1971 and 1982; Youd et al., 2001; Cetin et al., 2004; Idriss and Boulanger, 2004; Moss et al., 2006; Robertson, 2004 and 2009). In the analysis, peak ground accelerations (PGA) are estimated for scenario earthquakes of moment magnitudes at distances from the two possible sources by employing regionally appropriate ground motion prediction equations (GMPEs). In this study, medium GMPEs developed for use in the new generation of seismic hazard maps (Atkinson and Boore, 2011; Atkinson et al., 2012; Atkinson and Assatourians, 2012) are used to calculate peak ground accelerations for the scenario earthquakes. After determining the accelerations, cyclic stress ratios (CSR) generated by scenario earthquakes are calculated using Equation 1,

$$CSR_{7.5} = \frac{\tau_{ave}}{\sigma'_{vo}} = 0.65 \cdot \left(\frac{a_{max}}{g}\right) \cdot \left(\frac{\sigma_{vo}}{\sigma'_{v0}}\right) \cdot r_d \cdot \frac{1}{MSF} \quad (1)$$

where a_{max}=PGA (horizontal component), (a_{max}/g) is PGA divided by the acceleration due to gravity; σ_{vo} and σ'_{v0} are the total and effective vertical overburden stresses, respectively; r_d is a stress reduction coefficient; and MSF is the magnitude scaling factor. The $CSR_{7.5}$ represents the normalized shear stress (τ_{ave}/σ_v) induced in the soil by the earthquake event (i.e., the seismic demand) and commonly referenced to a benchmark case with **M** = 7.5.

Variations in standard penetration test (SPT) procedure are corrected by adjusting the measured blow count (N_m) using Equation 2:

$$\boldsymbol{N_{1(60)} = C_N\, C_E\, C_B\, C_R\, C_S\, N_m} \quad (2)$$

where $N_{1(60)}$ is normalized blow count corrected for hammer energy (C_E), effective confining stress (C_N), borehole diameter (C_B), rod length (C_R), and sampler configuration (C_S), with N_m being the measured SPT resistance or "blow count" reported in blows/foot (or blows/0.3m). In this way, the measured N value is standardized to 60% of the potential energy.

Following the computations of the cyclic stress ratio and the adjusted and normalized blow count, the liquefaction potential of representative layers at borehole sites is determined by plotting CSR versus normalized blow count [$(N_1)_{60}$] for **M** 7.5 earthquakes. If CSR is greater than or equal to CRR, the value plots on or above the curve, and the soil is likely to liquefy. Conversely, if CSR is less than CRR, the value plots below the curve, and liquefaction is considered unlikely.

In this study, we use the approximation to the base curve. For clean sands, which are tested in boreholes using the SPT, CRR for an **M** 7.5 event proposed by Youd et al. (2001) is given by Equation 3:

$$CRR_{7.5} = \frac{1}{34 - (N_1)_{60-cs}} + \frac{(N_1)_{60-cs}}{135} + \frac{50}{\left[10\,.\,(N_1)_{60-cs} + 45\right]^2} - \frac{1}{200} \qquad (3)$$

for $(N_1)_{60\text{-}cs} < 30$; $(N_1)_{60\text{-}cs}$ refers to equivalent clean sand.

The CRR for magnitudes other than 7.5 is calculated by multiplying $CSR_{7.5}$ by the appropriate magnitude scaling factor (MSF), which is given by Equation 4 where M_w represents moment magnitude:

$$MSF = (M_w/7.5)^{-3.3} \qquad (4)$$

As a means to better quantify uncertainty, stress-based methods have been re-evaluated using probabilistic analysis. In lieu of a single CRR curve, a family of CRR curves is derived to indicate the probability of liquefaction (P_L). Sets of probability curves have been developed for the SPT with ranges generally given from $P_L = 5\%$ up to $P_L = 95\%$ (Liao et al., 1988; Youd and Noble, 1997; Toprak et al., 1999; Juang et al., 2002; Cetin et al., 2004; Boulanger and Idriss, 2012).

Alternatively, the calculated factor of safety (FS) can be used to approximately assess the P_L. For example, in their approach, Juang and Jiang (2000) suggest (Equation 5):

$$P_L = \frac{1}{1 + (FS\ /\ 1.0)^{3.34}}, \qquad (5)$$

where P_L is the probability of liquefaction. If P_L is greater than or equal to 50%, a layer is likely to liquefy. This approach is taken in this study due to its simplicity and ease of use in spread sheets.

In order to calculate liquefaction potential, the depth and relative density of sandy soils or sediment must be known. We gleaned this information from borehole logs previously collected by the Virginia Department of Transportation at bridge sites along portions of the rivers where we found and documented liquefaction features. Information about the sites, including the borehole location map identification numbers (Map ID) shown on Figures 1 and 2 are given in

Table 5. The distance between earthquake sources and the borehole locations are provided in Table 6. Descriptions of the sediment at the sites are provided in Appendix A. In the analysis, we used a water table depth of 3 m based on observations in boreholes and the likelihood that the water table was somewhat deeper at the time of the paleoearthquake than it is today.

Table 5. Locations of geotechnical data used in liquefaction potential analysis.

Site Name (Map ID)	Latitude N (Dec. Degrees)	Longitude W (Dec. Degrees)	Location Description
Rivanna River (1)	37.91846	78.29778	Rt. 600 bridge near Lake Monticello
So. Anna River 1 (2)	37.89553	77.93331	Rt. 699 bridge southeast of Mineral
So. Anna River 1 (3)	37.79233	7.83068	Rt. 610 bridge southwest of Montpelier
James River (4)	37.57678	77.67938	Rt. 288 bridge west of Richmond
Pamunkey River 1 (5)	37.78883	77.36994	Rt. 301 bridge north of Hanover
Pamunkey River 2 (6)	37.71531	77.28918	Rt. 615 bridge southeast of Hanover
Mattaponi River (7)	37.94221	77.32048	Rt. 654 bridge south of Bowling Green

Table 6. Distance (km) between earthquake sources and geotechnical sites used in analysis.

Scenario Earthquake Source	Rivanna River	So. Anna River 1	So. Anna River 2	James River	Pamunkey River 1	Pamunkey River 2	Mattaponi River
2011 Mineral earthquake	30	10	20	45	55	65	58
Ashland area	78	45	35	33	10	16	18

Results of Analysis

The results of the evaluation of scenario earthquakes for two possible sources - a source near the 2011 Mineral, VA, earthquake and a source in the Ashland area - are discussed below. Detailed results of liquefaction potential analysis are provided in Appendix B and summarized in Tables 7 and 8 below.

Considering scenario earthquakes with a source similar to the 2011 Mineral earthquake, a **M** 5.5 earthquake would induce liquefaction at the local geotechnical site, South Anna River 1 (2), but not at any of the other sites (Table 7). It would take a **M** 6 earthquake to induce liquefaction also at South Anna River 2 (3) at a distance of 20 km. These two results agree with observations following the 2011 **M** 5.7 Mineral earthquake that induced liquefaction only in the epicentral area. This finding indicates that the analysis is providing meaningful results, though it should be noted that uncertainties in magnitude estimates can range from 0.25-0.5 magnitude units.

For other scenario events with a source similar to the 2011 Mineral earthquake, a **M** 6.25 earthquake would induce liquefaction at Rivanna River (1); a **M** 6.5 earthquake would induce liquefaction at Pamumkey River 1 (5); a **M** 6.75 earthquake would induce liquefaction at James River (4) and Pamumkey River 2 (6); and a **M** 7.0 earthquake would be required to induced liquefaction at the Mattaponi River (7).

Considering scenario earthquakes with a source near Ashland, a **M** 5.5 earthquake would induce liquefaction at both Pamunkey River 1 (5) and Pamunkey River 2 (6), but not at any of the other sites (Table 8). It would take a **M** 6.0 earthquake to induce liquefaction at Mattaponi River (7); a **M** 6.25 earthquake would induce liquefaction at South Anna River 2 (3); a **M** 6.5 earthquake would induce liquefaction at South Anna River 1 (2) and the James River (4); and a **M** 6.75 earthquake would be required to induce liquefaction at Rivanna River (1).

As discussed in the section, Interpretation of Timing, Locations, and Magnitudes of Earthquakes, there are at least two generations of liquefaction features that formed in the CVSZ prior to the 2011 Mineral earthquake: a younger generation that formed during the past 350 years and an older generation that formed between 350-2800 years ago. The 1875 **M** 4.8 ± 0.2 earthquake was likely responsible for younger generation of features. During this analysis, we did not evaluate scenario earthquakes of **M** 4.8-5.5 at distances of 10-20 km which would have helped to constrain the location and magnitude of the historic earthquake that caused liquefaction on the James and Pamunkey Rivers.

Based on similarity in weathering characteristics and lack of cross-cutting relationships, the older generation of features is thought to have formed during one paleoearthquake, although multiple events cannot be ruled. According to this analysis, such a paleoearthquake, if produced by the 2011 Mineral earthquake source, would have to be of **M** 7.0 to induce liquefaction at the sites on the Mattaponi, Pamunkey, South Anna, and Rivanna Rivers. If it were produced by a source near Ashland, the paleoearthquake would have to be of **M** 6.75 to induce liquefaction at the same sites.

A magnitude estimate of **M** 7.0 for a paleoearthquake produced by the Mineral source is 1.0 magnitude unit greater than the estimate of **M** ≥ 6 derived from the magnitude-distance relation; whereas, the magnitude estimate of **M** 6.75 for a paleoearthquake produced by the Ashland source is only 0.25 magnitude unit greater than the estimate of **M** ≥ 6.5 derived from the magnitude-distance relation. It is not surprising that the magnitude estimates based on liquefaction potential analysis are greater than those derived from the magnitude-distance relation. The liquefaction potential analysis uses blow counts (related to soil density and liquefaction susceptibility) measured at the geotechnical sites; whereas, the magnitude-distance relation is based on liquefaction in very susceptible sediment. The two magnitude estimates for a paleoearthquake produced by the Ashland source, however, are in much closer agreement than the magnitude estimates for a paleoearthquake produced by the Mineral source. This suggests that the paleoearthquake was more likely located near Ashland than Mineral. As stated before, an earthquake location near Ashland also would help to explain the larger size of liquefaction features on the Pamunkey and Mattaponi Rivers. For an earthquake located near Mineral to induce liquefaction at the sites on the Mattaponi and Pamunkey Rivers, it would have to be very

Table 7. Summary of evaluation of 2011 Mineral scenario earthquakes.

Site Name	Map ID	Distance (km)	Results[1]
1. Scenario earthquake M 5.5			
South Anna River 1	2	10	L
South Anna River 2	3	20	N
Rivanna River	1	30	N
James River	4	45	N
Pamunkey River 1	5	55	N
2. Scenario earthquake M 5.75			
South Anna River 2	3	20	N
Rivanna River	1	30	N
James River	4	45	N
Pamunkey River 1	5	55	N
3. Scenario earthquake M 6.0			
South Anna River 2	3	20	L
Rivanna River	1	30	N
James River	4	45	N
Pamunkey River 1	5	55	N
4. Scenario earthquake M 6.25			
Rivanna River	1	30	L
James River	4	45	N
Pamunkey River 1	5	55	N
5. Scenario earthquake M 6.5			
James River	4	45	L/N
Pamunkey River 1	5	55	L
Mattaponi River	7	58	N
Pamunkey River 2	6	65	N
6. Scenario earthquake M 6.75			
James River	4	45	L
Mattaponi River	7	58	N
Pamunkey River 2	6	65	L
6. Scenario earthquake M 7.0			
Mattaponi River	7	58	L

[1] L = Liquefaction likely for 45% - 100% of the layers analyzed; L/N = marginal because liquefaction predicted for 24% - 44% of the layers analyzed; N = liquefaction not likely because liquefaction predicted for less than 24% of the layers analyzed.

Table 8. Summary of evaluation of Ashland area scenario earthquakes.

Site Name	Map ID	Distance (km)	Results
1. Scenario earthquake M 5.5			
Pamumkey River 1	5	10	L
Pamunkey River 2	6	16	L
Mattaponi River	7	18	N
South Anna River 2	3	35	N
South Anna River 1	2	45	N
2. Scenario earthquake M 5.75			
Mattaponi River	7	18	N
South Anna River 2	3	35	N
South Anna River 1	2	45	N
3. Scenario earthquake M 6.0			
Mattaponi River	7	18	L
James River	4	33	N
South Anna River 2	3	35	N
South Anna River 1	2	45	N
Rivanna River	1	78	N
4. Scenario earthquake M 6.25			
James River	4	33	L/N
South Anna River 2	3	35	L
South Anna River 1	2	45	N
Rivanna River	1	78	N
5. Scenario earthquake M 6.5			
James River	4	33	L
South Anna River 1	2	45	L
Rivanna River	1	78	N
6. Scenario earthquake M 6.75			
Rivanna River	1	78	L

[1] L = Liquefaction likely for 45% - 100% of the layers analyzed; L/N = marginal because liquefaction predicted for 24% - 44% of the layers analyzed; N = liquefaction not likely because liquefaction predicted for less than 24% of the layers analyzed

large (**M** 7.0). Such a large earthquake would have produced larger liquefaction features on the South Anna River. Alternatively, the distribution of paleoliquefaction features could be explained by two smaller earthquakes. A **M** 6.25 earthquake produced by the Mineral source

could be responsible for the features on the South Anna and Rivanna Rivers, and a **M** 6.0 earthquake produced by the Ashland source could have led to the formations of the features on the Pamunkey and Mattaponi Rivers. However, given the similarity in the blow counts (N) of sediments at the South Anna, Pamunkey, and Mattaponi sites (see Table A-1 in Appendix A), a larger magnitude earthquake near Ashland better explains the formation of larger liquefaction features along the Pamunkey and Mattaponi Rivers.

Conclusions

During a paleoliquefaction study conducted in 2015, liquefaction features were found and studied along five rivers in the CVSZ: the South Anna River southeast of the epicenter of the 2011 **M** 5.7 Mineral earthquake, Stigger Creek, a tributary to the Rivanna River, west of the epicenter, the James River south of the epicenter, and the Mattaponi and Pamunkey Rivers east of the Fall Line (Tuttle et al., 2015; Tuttle, 2016; Carter et al., 2016). On the basis of their weathering characteristics as well as dating of sediments in which they occur, the liquefaction features were attributed to at least two episodes of earthquake-induced liquefaction. A few small (≤ 3 cm) sand dikes and strata-bound soft-sediment deformation structures at three sites on the James and Pamunkey Rivers were interpreted to have formed during a recent earthquake in the past 500 years. Bioturbated and weathered sand dikes (≤ 7 cm) and sills along the Mattaponi, Pamunkey, and South Anna Rivers, as well as the Rivanna River (Stigger Creek), were interpreted to be prehistoric in age and to have formed during an earthquake in the past 4,500 years. Based on the size and areal distribution of the liquefaction features, the paleoearthquake was interpreted to be of **M** ≥ 6 and to be located east of the 2011 Mineral earthquake.

During this study, thirteen additional sand dikes and soft-sediment deformation features were found and studied at six sites up to 75 km east from the epicenter of the 2011 Mineral earthquake. These features were found during systematic surveys of cutbank exposures along 30 km of the Mattaponi River and 39 km of the Pamunkey River east of the Fall Line (Figure 7). A survey also was conducted along 8 km of the James River but no additional liquefaction feature was found. The lack of prehistoric liquefaction features along the James River may be due to the relatively young age of sediments exposed in the river cutbanks.

The newly found liquefaction features along the Mattaponi and Pamunkey Rivers include sand dikes, ranging up to 20 cm wide, composed of coarse-fine sand with small pebbles and silt clasts as well as sand dipairs, foundered clasts, and disturbed bedding. All the sand dikes and diapirs intrude mottled silt or sandy silt, some of the dikes branch upward, and all of the dikes appear to pinch upward. The upper portion of most of the dikes are bioturbated and mottled suggesting that they are paleoin age. Radiocarbon dating of charred material collected from sand layers below the sand dikes and from mottled silt intruded by the dikes and diapirs provides maximum constraining ages, not necessarily close maximum constraining ages, for the liquefaction features that range from 2730 yr B.P. to 7160 yr B.P. Unfortunately, there are no minimum constraining ages to help bracket and narrow age estimates of the features. Given the similarity in their weathering characteristics and the lack of cross-cutting relationships, the paleoliquefaction features found during this study, as well as those studied in 2015, are interpreted to have formed during one paleoearthquake. Using the youngest maximum constraining age, these features likely formed since 2730 yr B.P., or between 350-2800 years ago. This age estimate is supported

by sea level during the Late Holocene. Along the Virginia Eastern Shore, sea level was more than 3 m lower relative to today prior to 2800 yr B.P. and 5.5 m lower relative to today prior to 4000 yr B.P. Lower sea level may have reduced the liquefaction susceptibility of sediment along the coastal rivers. Therefore, earthquake-induced liquefaction features are more likely to have formed during the Late Holocene, and there may be large gaps in the paleoliquefaction record during the Middle and Early Holocene.

The paleoliquefaction features are larger, more numerous, and more broadly distributed than the historical features. The largest features occur on the Pamunkey and Mattaponi Rivers, suggesting that the earthquake source may be located nearby, perhaps in the Ashland area where a cluster of small earthquakes have been recorded since 1974. According to the relation between earthquake magnitude and greatest distance to liquefaction (Castilla and Audemard, 2007), a **M** ≥ 6.5 paleoearthquake centered near Ashland could explain the distribution of features across the region. Evaluation of scenario earthquakes using liquefaction potential analysis, found that a **M** 6.75 produced by a source near Ashland would induce liquefaction at sites along the Mattaponi, Pamunkey, South Anna, and Rivanna Rivers. The analysis also found that a **M** 7.0 earthquake would be required to induce liquefaction at all the sites if it were produced by the 2011 Mineral earthquake source. A **M** 6.75 produced by a source near Ashland is in closer agreement with the estimate based on the magnitude-distance relation and better explains the size variation as well as the regional distribution of liquefaction features. Alternatively, a **M** 6.25 earthquake produced by the Mineral source and a **M** 6.0 earthquake produced by the Ashland source might explain the distribution of paleoliquefaction features, but would not account for the larger paleoliquefaction features along the Mattaponi and Pamunkey Rivers.

During this study, the age estimate of the historic liquefaction features previously found on the James River and Pamunkey Rivers was further narrowed. Using the youngest maximum constraining age, these features likely formed since 280 yr B.P., or during the past 350 years. The 1875 **M** 4.8 ± 0.2 and MMI VII earthquake is the largest historical event to strike the area and the most likely candidate to have induced liquefaction on the James and Pamunkey Rivers. The assigned earthquake location is about 28 km northwest of the James River liquefaction sites. According to the magnitude and distance relation, the 1875 would not have induced liquefaction at the James River sites if it were of **M** 4.8 ± 0.2 and located 28 km away. At that distance, the earthquake would have to be of **M** 5.5 to induce liquefaction at the James River liquefaction sites. Other alternatives include a **M** ≥ 5 earthquake located between the James and Pamunkey Rivers or a **M** 4.8 within 15 km of the James River sites and another small earthquake in close proximity to the Pamunkey River site. Unfortunately, scenario earthquakes of **M** < 5.5 were not evaluated for the James and Pamunkey Rivers but will be included in future analyses.

More searching, measuring, and dating of liquefaction features beyond their currently known distribution is needed to improve our understanding of the number, timing, location, and magnitude of past earthquakes in the CVSZ. Special attention should be given to weathering characteristics and minimum constraining ages of liquefaction features. Also, evaluation of additional scenario earthquakes, including events of **M** □□5.5, is needed to assess alternative locations and magnitudes of earthquakes responsible for the liquefaction features.

Acknowledgments

Kathleen Dyer-Williams performed liquefaction potential analysis for scenario earthquakes using geotechnical data provided by Carl Benson and Mike Hall of the Virginia Department of Transportation (VDOT) and downloaded from the VDOT website. Kathy Tucker provided locations and magnitudes of instrumentally recorded earthquakes as well as updated the regional paleoliquefaction database and the CVSZ map showing liquefaction sites, mapped faults, and surficial geology. Laurel Bauer, Zamara Fuentes, and Carlos Velez participated in river surveys for liquefaction features. Beta Analytic, Inc. performed radiocarbon dating of organic samples collected during field work. This project was conducted in cooperation with Mark Carter of the U.S. Geological Survey. The material in this report is based upon work supported by the U.S. Geological Survey under Grant No. G18AP00027.

References Cited

Atkinson, G., and Boore, D., 2011, Modification to existing ground-motion prediction equations in light of new data, Bulletin of the Seismological Society of America, v. 101, n. 3, p. 1121-1135.

Atkinson, G., (with input from) J. Adams, G. Rogers, T. Onur, and K. Assatourians, 2012, White paper on development of ground motion prediction equations for Canadian national seismic hazard maps, www.seismotoolbox.ca (Miscellaneous Resources).

Atkinson, G., (Project Leader), K. Assatourians, 2012, GMPEs for national hazard maps, *www.seismotoolbox.ca* (Miscellaneous resources).

Bollinger, G. A., Chapman, M. C., Sibol, M. S., and Costain, J. K., 1985, An analysis of earthquake focal depth in the southeastern U.S., Geophysical Research Letters, v. 12, p. 785-788.

Boulanger, R. W., and Idriss, I. M., 2012, Probabilistic standard penetration test-based liquefaction: triggering procedure, J. Geotechnical and Geoenvironmental Engineering, v. 138, n. 10, p. 1185-1195.

Carter, M. W., 2015, Characterizing pedogenic and potential paleoseismic features in South Anna River alluvium: epicentral region of the 2011 earthquake Central Virginia seismic zone, Presentation at the 2015 Virginia Geological Research Symposium.

Carter, M. W., Tuttle, M. P., and Dunahue, J., 2016, Characteristics of paleoliquefaction features in the Central Virginia seismic zone, Geological Society of America, Abstracts with Programs, v. 48, n. 3, doi: 10.1130/abs/2016SE-273045.

Castilla, R. A., and Audemard, F. A., 2007, Sand blows as a potential tool for magnitude estimation of pre-instrumental earthquakes, Journal of Seismology, v. 11, p. 473-487.

Cetin, K. O., Seed, R. B., Der Kiureghian, A., Tokimatsu, K., Harder, L. F. Jr, Kayen, R. E., Moss, R. E. S., 2004, SPT-based probabilistic and deterministic assessment of seismic soil liquefaction potential, ASCE Journal of Geotechnical and Environmental Engineering, v. 130, n. 12, p. 1314-1340.

Chapman, M. C., 2015, Magnitude, recurrence interval, and near-source ground motion modeling of the Mineral, Virginia, earthquake of 23 August 2011, *in* Horton, J. W., Jr., Chapman, M. C., and Green, R. A., eds., The 2011 Mineral, Virginia, earthquake, and its significance for seismic hazards in eastern North America: Geological Society of America Special Paper 509, p. 27-4.

Dominion, 2004, Response to request for additional information no. 3, North Anna Early Site Permit Application, Dominion Nuclear North Anna, LLC, U.S. Nuclear Regulatory Commission, Report ML042800292, 110 p.

Ebel, J. E., Bonjer, K., and Oncescu, M., 2000, Paleoseismicity: seismicity evidence for past large earthquakes, Seismological Research Letter, v. 71, p. 283-294; doi:10.1785/gssrl.71.2.283.

Ellsworth, W. L., Imanishi, K., Luetgert, J. H., and Pratt, T. L., 2011, The Mw 5.8 Virginia earthquake of August 23, 2011: A high stress drop event in a critically stressed crust, Abstract, 83rd Annual Meeting of the Eastern Section of the Seismological Society of America, October, 2011, Little Rock, Arkansas, p. 40.

Eppley, R. A., 1965, Earthquake history of the United States, Part I: stronger earthquakes of the United States: U.S. Coast and Geo- detic Survey, Washington, D.C., 120 p.

Green, R. A., Obermeier, S. F., Olson, S. M., 2005, Engineering geologic and geotechnical analysis of paleoseismic shaking using liquefaction effects: field examples, Eng. Geol., v. 76, p. 263-293.

Green, R., Lasley, S., Carter, M. W., Munsey, J. W., Maurer, B. W., Tuttle, M. P., 2015, Geotechnical aspects in the epicentral region of the 2011 Mw 5.8 Mineral, Virginia, earthquake, in Horton, J.W., Jr., Chapman, M.C., and Green, R.A., eds., The 2011 Mineral, Virginia, earthquake, and its significance for seismic hazards in eastern North America: Geological Society of America Special Paper 509, doi:10.1130/2015.2509(09).

Hopper, M. G. and Bollinger, G. A., 1971, Virginia's two largest earthquakes-December 22, 1875 and May 31, 1897, Bulletin of the Seismological Society of America, v. 61, n. 4, p. 1033-1039.

Horton, J. W., Jr., and Williams, R. A., 2012, The 2011 Virginia earthquake: What are scientists learning?, Transactions, American Geophysical Union, EOS, v. 93, n. 33, p.317-318.

Horton, J. W., Chapman, M. C., and Green, R. A., 2015, The 2011 Mineral, Virginia, earthquake, and its significance for seismic hazards in eastern North America-Overview and synthesis, *in* Horton, J. W., Jr., Chapman, M. C., and Green, R. A., eds., The 2011 Mineral, Virginia, earthquake, and its significance for seismic hazards in eastern North America: Geological Society of America Special Paper 509, p. 1-25.

Hughes, K. S., Hibbard, J. P., and Bohnenstiehl, D. R., 2015, Relict Paleozoic faults in the epicentral area of the August 23, 2011 central Virginia earthquake: Assessing the relationship between preexisting strain and modern seismicity, *in* Horton, J. W., Jr., Chapman, M. C., and Green, R. A., eds., The 2011 Mineral, Virginia, earthquake, and its significance for seismic hazards in eastern North America: Geological Society of America Special Paper 509, p. 331-343.

Idriss, I.M., and Boulanger, R.W., 2004, Semi-empirical procedures for evaluating liquefaction potential during earthquakes, Proc., 11th International Conference on Soil Dynamics and Earthquake Engineering, and 3rd International Conference on Earthquake Geotechnical Engineering, D. Doolin et al., eds., Stallion Press, v. 1, p. 32-56.

Juang, C. H., and Jiang, T., 2000, Assessing probablistic methods for liquefaction potential evaluation, Soil Dynamics and Liquefaction 2000, GSP 107 (Proceedings GeoDenver), American Society of Civil Engineers, Reston, VA.

Juang, C. H., Jiang, T., and Andrus, R. D., 2002, Assessing probability-based methods for liquefaction potential evaluation, Journal of Geotechnical and Geoenvironmental Engineering, v. 128, n. 7, p. 580-589.

Liao, S. S. C., Veneziano, D., and Whitman, R. V., 1998, Regression models for evaluating liquefaction probability, Journal of Geotechnical Engineering, v. 114, n. 4, p. 389–411.

Mixon, R. B., and Newell, W. L., 1977, Stafford fault system: Structures documenting Cretaceous and Tertiary deformation along the Fall Line in northeastern Virginia, Geology, v. 5, p. 437-440.

Mixon, R. B., Berquist, C. R., Jr., Newell, W. L., Johnson, G. H., Powars, D. S., Schindler, J. S., and Rader, E. K., 1989, Geologic map and generalized cross sections of the Coastal Plain and adjacent parts of the Piedmont, Virginia: U.S. Geological Survey Miscellaneous Investigations Series Map 1-2033, 2 sheets, scale 1:250,000.

Mixon, R. B., Pavlides, L., Powars, D. S., Froelich, A. J., Weems, R. E., Schindler, J. S., Wayne, W. L., Edwards, L. E., and Ward, L. W., 2000, Geologic Map of the Fredericksburg 30' x 60' Quadrangle, Virginia and Maryland, U.S. Geological Survey Miscellaneous Investigations Series Map 1-2607, 2 sheets, scale 1:100,000, 34 p.

Moss, R. E. S., Seed, R. B., Kayen, R. E., Steward, J. P., Der Kiureghian, and Cetin, K. O., 2006, CPT-based probablistic and deterministic assessment of in-situ seismic soil liquefaction potential, J. Geotechnical & Geoenvironmental Engineering, v. 132, n. 8, p. 1032-1051

Oaks, S. D. and Bollinger, G. A., 1986, The Epicenter of the mb 5, December 22, 1875 Virginia earthquake: New findings from documentary sources: Seismological Research Letters, v. 57, no. 3, p. 65–75.

Obermeier, S. F., 1996, Using liquefaction-induced features for paleoseismic analysis, *in* McCalpin, J. P., ed., Paleoseismology, Academic Press, San Diego, CA, p. 331-396.

Obermeier, S. F., and McNulty, W. E., 1998, Paleoliquefaction evidence for seismic quiescence in central Virginia during late and middle Holocene time, EOS, Transactions of the American Geophysical Union, v. 79, no. 17, Spring Meeting Supplement, Abstract T41A-9.

Olson S. M., Green, R. A., and Obermeier, S. F., 2005, Geotechnical analysis of paleoseismic shaking using liquefaction features: A major updating, Engineering Geology, v. 76, p. 235–261.

Petersen, M. D., Frankel, A. D., Harmsen, S. C., Mueller, C. S., Haller, K. M., Wheeler, R. L., Wesson, R. L., Zeng, Y., Boyd, O. S., Perkins, D. M., Luco, N., Field, E. H., Wills, C. J., and Rukstales, K. S., 2008, Documentation for the 2008 update of the United States National Seismic Hazard Maps, U.S. Geological Survey Open-File Report 2008-1128, 61 p.

Powars, D. S., Horton, J. W., Jr., 2010, Coastal Plain faults rooted in crystalline basement across the Salisbury Embayment, Geological Society of America Abstracts with Programs, v. 42, n. 5, p. 219.

Powars, D. S., Catchings, R. D., Horton, J. W., Jr., 2012, Stafford fault system: Investigating paleoseismicity in Virginia, Geological Society of America Abstracts with Programs, v. 44, n. 7, p. 593.

Powars, D. S., Catchings, R. D., Horton, J. W., Jr., Schindler, S., and Pavich, M. J., 2015, Stafford fault system: 120 million year fault movement history of northern Virginia, *in* Horton, J. W., Jr., Chapman, M. C., and Green, R. A., eds., The 2011 Mineral, Virginia, earthquake, and its significance for seismic hazards in eastern North America: Geol. Soc. Am., Special Paper 509, p. 407-431.

Pratt T. L., Coruh, C. Costain, J. K., and Glover, L., III, 1988, A geophysical study of the Earth's crust in central Virginia: Implication for Appalachian crustal structure, Journal Geophysical Research, v. 93, n. B6, p. 6649-6667.

Pratt, T. L., Horton, J. W., Spears, D. B., Gilmer, A. K., and McNamara, D. E., 2015, The 2011 Virginia **M**5.8 earthquake: Insights from seismic reflection imaging into influence of older structures on eastern U.S. seismicity, *in* Horton, J. W., Jr., Chapman, M. C., and Green, R. A., eds., The 2011 Mineral, Virginia, earthquake, and its significance for seismic hazards in eastern North America: Geological Society of America Special Paper 509, p. 285-293.

Robertson, P. K., 2004, Evaluating soil liquefaction and post-earthquake deformations using the CPT, Geotechnical and Geophysical Site Characterization, v.1 (Proc. ISC-2, Porto), Millpress, Rotterdam, p. 233-252.

Robertson, P. K., 2009, Interpretation of cone penetration tests: a unified approach, Canadian Geotechnical Journal, v. 46, n. 11, p. 1335-1355.

Schindler, J. S., Harrison, R. W., and Obermeier, S. F., 2012, Review and update of paleoliquefaction evidence for Holocene seismic activity in the CVSZ, [abs.] Eastern Section, Seismological Society of America, Program and Abstracts, p. 43.

Seed, H. B. and Idriss, I. M., 1971, Simplified procedure for evaluating soil liquefaction potential. Journal of the Soil Mechanics & Foundations Division (ASCE), v. 97 (SM9), p. 1249-1273.

Seed, H. B., and Idriss, I. M., 1982, Ground motions and soil liquefaction during earthquakes, Earthquake Engineering Research Institute, Berkley, 134 p.

Soller, D. R., and Reheis, M. C., 2004, Surficial materials in the conterminous United States, U.S. Geological Survey, Open-file Report 03-275, scale 1:5,000,000, http://pubs.usgs.gov/of/2003/of03-275/.

Talma, A. S. and Vogel, J. C., 1993, A simplified approach to calibrating C14 dates, Radiocarbon, v. 35, p. 317-322.

Toprak, S., Holzer, T. L., Bennett, M. J., and Tinsley, J. J., 1999, CPT- and SPT-based probabilistic assessment of liquefaction potential, Proceedings of the 7th U.S.–Japan Workshop on Earthquake Resistant Design of Lifeline Facilities and Countermeasures Against Liquefaction, Seattle, WA, MCEER, Buffalo, NY, Technical Report MCEER-99-0019.

Tuttle, M. P., 2001, The use of liquefaction features in paleoseismology: Lessons learned in the New Madrid seismic zone, central United States, Journal of Seismology, v. *5*, p. 361-380.

Tuttle, M. P., 2016, Earthquake potential of the CVSZ, Final Technical Report, Prepared for U.S. Geological Survey grant G13AP00045, 32 p.

Tuttle, M., Law, T., Seeber, L., and Jacob, K., 1990, Liquefaction and ground failure in Ferland, Quebec, triggered by the 1988 Saguenay Earthquake, Canadian Geotechnical Journal, v. 27, p. 580-589.

Tuttle, M. P., Al-Shukri, H, and Mahdi, H., 2006, Very large earthquakes centered southwest of the New Madrid seismic zone 5,000-7,000 years ago, Seismological Research Letters, v. 77, n. 6, p. 664-678.

Tuttle, M. P., and Atkinson, G. M., 2010, Localization of large earthquakes in the Charlevoix seismic zone, Quebec, Canada during the past 10,000 years, Seismological Research Letters, v. 81, n. 1, p. 18-25.

Tuttle, M. P., and Busch, T. A., 2011, Post-earthquake survey following the 2011 M 5.8 Virginia event, Preliminary report to the U.S. Nuclear Regulatory Commission, 2 p.

Tuttle, M. P., and Hartleb, R., 2012, Central and eastern U.S. paleoliquefaction database, uncertainties associated with paleoliquefaction data, and guidance for seismic source characterization, Appendix E. *in* The Central and Eastern U.S. Seismic Source

Characterization for Nuclear Facilities, Technical Report, EPRI, Palo Alto, CA, U.S. DOE, and U.S. NRC, 135 p. plus database.
Tuttle, M., Carter, M. W., Dunahue, J., 2015, Paleoliquefaction study of the earthquake potential of the Central Virginia seismic zone, Geological Society of America, Abstracts with Programs, v. 47, n. 7, p. 466.
Tuttle, M. P., Hartleb, R., Wolf, L., and Mayne, P. W., 2019, Paleoliquefaction studies and the evaluation of seismic hazard, Geosciences, v. 9, n. 7, 61 p, doi:10.3390/geosciences9070311.
Van de Plassche, O., 1990, Mid-Holocene sea-level change on the Eastern Shore of Virginia, Marine Geology, v. 91., p. 149-154.
Vogel, J. C., Fuls, A., Visser, E., and Becker, B., 1993, Pretoria calibration curve for short-lived samples, Radiocarbon, v. 33, p. 73-86.
Wolin, E., Stein, S., Pazzaglia, F., Meltzer, A., Kafka, A., and Berti, C., 2012, Mineral, Virginia, earthquake illustrates seismicity of a passive-aggressive margin, Geophysical Research Letters, v. 39, L02305, doi:10.1029/2011GL050310.
Youd, T.L. and S.K. Noble, 1997, Liquefaction criteria based on statistical and probabilistic analyses, Proceedings, NCEER Workshop on Evaluation of Liquefaction Resistance of Soils, Salt Lake City, NCEER Technical Report No. 97-0022, p. 201-215.
Youd, T. L., and Idriss, I. M., 2001, Liquefaction resistance of soils: Summary report from the 1996 NCEER and 1998 NCEER/NSF workshops on evaluation of liquefaction resistance of soils, Journal of Geotechnical and Geoenvironmental Engineering, v. 127, n. 4, p. 297-313.

Bibliography of Related Publications

Carter, M. W., Tuttle, M. P., and Dunahue, J., 2016, Characteristics of paleoliquefaction features in the Central Virginia seismic zone, Geological Society of America, Abstracts with Programs, v. 48, n. 3, doi: 10.1130/abs/2016SE-273045.
Tuttle, M., 2015, Paleoliquefaction studies: learning from historical and modern cases of liquefaction and dating paleoliquefaction features, U.S. NRC Paleoliquefaction training workshop in the New Madrid seismic zone, U.S. NRC ADAMS.
Tuttle, M. P., and Busch, T. A., 2011, Post-earthquake survey following the 2011 **M** 5.8 Virginia event, Preliminary report to the U.S. Nuclear Regulatory Commission, 2 p.
Tuttle, M. P., and Hartleb, R., 2012, Central and eastern U.S. paleoliquefaction database, uncertainties associated with paleoliquefaction data, and guidance for seismic source characterization, Appendix E. *in* The Central and Eastern U.S. Seismic Source Characterization for Nuclear Facilities, Technical Report, EPRI, Palo Alto, CA, U.S. DOE, and U.S. NRC, 135 p. plus database.
Tuttle, M., Carter, M. W., Dunahue, J., 2015, Paleoliquefaction study of the earthquake potential of the Central Virginia seismic zone, Geological Society of America, Abstracts with Programs, v. 47, n. 7, p. 466.

Appendix A Sediment Used in Liquefaction Potential Analysis

Table A-1. Description of sediment used in liquefaction potential analysis

Site Name Borehole No. (Map ID)	Depth (m)	Description of Susceptible Sediment	Blow Count (N)[1]
Rivanna River BH 6 (1)	7.1 9.4	cohesionless sand gray sand with some silt	5 5
So. Anna River 1 BH31 (2)	4.0 5.0 7.0	yellow-brown silty sand, trace clay with fine to coarse gravel contains mica and thin roots, loose, moist yellow-brown silty sand, trace clay with fine to coarse gravel contains mica and thin roots, loose, moist dark, yellow-brown silty sand, contains mica, very loose	6 2 4
So. Anna River 2 BH10 (3)	8.0 9.0 11.0	micaceous, fine, wet sand with organics micaceous, fine, wet sand with organics micaceous, fine, wet, fine sand with organics	6 11 9
James River BH 7 (4)	4.2 5.3 6.3	sand, dark brown, wet, loose to dense sand, dark brown, wet, loose to dense sand, dark brown, wet, loose to dense	6 10 4
Pamunkey River 1 BH 2 (5)	4.5 6.1 7.6 9.1	gray sand gray sand gray gravelly sand gray gravelly sand	1 5 8 18
Pamunkey River 2 BH 1 (6)	6.6 7.7 8.6	gray sand with black heavy minerals gray sand with black heavy minerals gray sand with black heavy minerals	4 4 4
Mattaponi River BH 4 (7)	3.1 4.6	gray, fine, micaceous silty sand gray, fine, micaceous silty sand	3 8

[1] Blow count (N) is the total number of blows required to drive a split spoon sampler 0.3 m using standard hammer (63.5 kg) dropping 0.76 m.

Appendix B Results for Evaluation of Scenario Earthquakes

Table B-1a. Results of liquefaction potential analysis for M 5.5 scenario earthquake with similar source to 2011 Mineral earthquake

Site Name (Map ID)	Magnitude @ Distance (km)	amax[1]	Sediment Depth (m)	Blow Count[2]	Cyclic Stress Ratio[3]	Results (NL, L)[4]
So. Anna River 1	5.5 @ 10	0.32	4.0	6	0.237	N
(2)	5.5 @ 10	0.32	5.0	2	0.266	L
	5.5 @ 10	0.32	7.0	4	0.299	L
So. Anna River 2	5.5 @ 20	0.17	8.0	6	0.158	N
(3)	5.5 @ 20	0.17	9.0	11	0.161	N
	5.5 @ 20	0.17	11.0	9	0.162	N
Rivanna River	5.5@30	0.10	7.0	5	0.088	N
(1)	5.5@30	0.10	9.0	5	0.093	N
James River	5.5@45	0.06	4.0	6	0.046	N
(4)	5.5@45	0.06	5.0	10	0.051	N
	5.5@45	0.06	6.0	4	0.054	N
Pamunkey River 1	5.5@55	0.05	5.0	1	0.038	N
(5)	5.5@55	0.05	6.0	5	0.043	N
	5.5@55	0.05	8.0	8	0.045	N
	5.5@55	0.05	9.0	18	0.047	N

1. amax = Maximum acceleration at ground surface;

2. Blow Count = Total number of blows required to drive split spoon sampler 0.3 m using standard hammer (63.5 kg) dropping 0.76 m;

3. Cyclic Stress Ratio = Shear Stress induced in the soil causing liquefaction;

4. N= Liquefaction not likely; L = Liquefaction likely

Table B-1b. Results of liquefaction potential analysis for M 5.75 scenario earthquake with similar source to 2011 Mineral earthquake

SiteName (Map ID)	Magnitude @ Distance (km)	amax[1]	Sediment Depth (m)	Blow Count[2]	Cyclic Stress Ratio[3]	Results (NL, L)[4]
So. Anna River 2	5.75 @ 20	0.21	8.0	6	0.198	N
(3)	5.75 @ 20	0.21	9.0	11	0.202	N
	5.75 @ 20	0.21	11.0	9	0.204	N
Rivanna River	5.75@30	0.12	7.0	5	0.111	N
(1)	5.75@30	0.12	9.0	5	0.118	N
James River	5.75 @ 45	0.08	4.0	6	0.061	N
(4)	5.75 @ 45	0.08	5.0	10	0.066	N
	5.75 @ 45	0.08	6.0	4	0.071	N
Pamunkey River 1	5.75 @ 55	0.06	5.0	1	0.049	N
(5)	5.75 @ 55	0.06	6.0	5	0.056	N
	5.75 @ 55	0.06	8.0	8	0.059	N
	5.75 @ 55	0.06	9.0	18	0.061	N

1. amax = Maximum acceleration at ground surface;
2. Blow Count = Total number of blows required to drive split spoon sampler 0.3 m using standard hammer (63.5 kg) dropping 0.76 m;
3. Cyclic Stress Ratio = Stress causing liquefaction;
4. N= Liquefaction not likely; L = Liquefaction likely

Table B-1c. Results of liquefaction potential analysis for M 6 scenario earthquake with similar source to 2011 Mineral earthquake

Site Name (Map ID)	Magnitude @ Distance (km)	amax[1]	Sediment Depth (m)	Blow Count[2]	Cyclic Stress Ratio[3]	Results (NL, L)[4]
So. Anna River 2 (3)	6 @ 20	0.27	8.0	6	0.249	L
	6 @ 20	0.27	9.0	11	0.253	L
	6 @ 20	0.27	11.0	9	0.256	L
Rivanna River (1)	6 @ 30	0.16	7.0	5	0.143	N
	6 @ 30	0.16	9.0	5	0.151	N
James River (4)	6 @ 45	0.10	4.0	6	0.077	N
	6 @ 45	0.10	5.0	10	0.085	N
	6 @ 45	0.10	6.0	4	0.091	N
Pamunkey River 1 (5)	6 @ 55	0.08	5.0	1	0.063	N
	6 @ 55	0.08	6.0	5	0.071	N
	6 @ 55	0.08	8.0	8	0.076	N
	6 @ 55	0.08	9.0	18	0.078	N

1. amax = Maximum acceleration at ground surface;

2. Blow Count = Total number of blows required to drive split spoon sampler 0.3 m using standard hammer (63.5 kg) dropping 0.76 m;

3. Cyclic Stress Ratio = Shear Stress induced in the soil causing liquefaction;

4. N= Liquefaction not likely; L = Liquefaction likely

Table B-1d. Results of liquefaction potential analysis for M 6.25 scenario earthquake with similar source to 2011 Mineral earthquake

Site Name (Map ID)	Magnitude @ Distance (km)	amax[1]	Sediment Depth (m)	Blow Count[2]	Cyclic Stress Ratio[3]	Results (NL, L)[4]
Rivanna River (1)	6.25 @ 30	0.20	7.0	5	0.179	N
	6.25 @ 30	0.20	9.0	5	0.189	L
James River (4)	6.25 @ 45	0.13	4.0	6	0.099	N
	6.25 @ 45	0.13	5.0	10	0.108	N
	6.25 @ 45	0.13	6.0	4	0.116	N
Pamunkey River 1 (5)	6.25 @ 55	0.10	5.0	1	0.080	N
	6.25 @ 55	0.10	6.0	5	0.090	N
	6.25 @ 55	0.10	8.0	8	0.095	N
	6.25 @ 55	0.10	9.0	18	0.098	N

1. amax = Maximum acceleration at ground surface;

2. Blow Count = Total number of blows required to drive split spoon sampler 0.3 m using standard hammer (63.5 kg) dropping 0.76 m;

3. Cyclic Stress Ratio = Shear Stress induced in the soil causing liquefaction;

4. N= Liquefaction not likely; L = Liquefaction likely

Table B-1e. Results of liquefaction potential analysis for M 6.5 scenario earthquake with similar source to 2011 Mineral earthquake

Site Name Map ID #	Magnitude @ Distance (km)	amax[1]	Sediment Depth (m)	Blow Count[2]	Cyclic Stress Ratio[3]	Results (NL, L)[4]
James River (4)	6.5 @ 45	0.17	4.0	6	0.124	N
	6.5 @ 45	0.17	5.0	10	0.136	N
	6.5 @ 45	0.17	6.0	4	0.145	L
Pamunkey River 1 (5)	6.5 @ 55	0.13	5.0	1	0.101	L
	6.5 @ 55	0.13	6.0	5	0.114	L
	6.5 @ 55	0.13	8.0	8	0.121	N
	6.5 @ 55	0.13	9.0	18	0.124	N
Mattaponi River (7)	6.5 @ 58	0.12	3.0	3	0.077	N
	6.5 @ 58	0.12	5.0	8	0.093	N
Pamunkey River 2 (6)	6.5 @ 65	0.11	7.0	4	0.099	N
	6.5 @ 65	0.11	8.0	4	0.103	N
	6.5 @ 65	0.11	9.0	4	0.105	N

1. amax = Maximum acceleration at ground surface;

2. Blow Count = Total number of blows required to drive split spoon sampler 0.3 m using standard hammer (63.5 kg) dropping 0.76 m;

3. Cyclic Stress Ratio = Shear Stress induced in the soil causing liquefaction;

4. N= Liquefaction not likely; L = Liquefaction likely

Table B-1f. Results of liquefaction potential analysis for M 6.75 scenario earthquake with similar source to 2011 Mineral earthquake

Site Name Map ID #	Magnitude @ Distance (km)	amax[1]	Sediment Depth (m)	Blow Count[2]	Cyclic Stress Ratio[3]	Results (NL, L)[4]
James River	6.75 @ 45	0.21	4.0	6	0.157	L
(4)	6.75 @ 45	0.21	5.0	10	0.171	N
	6.75 @ 45	0.21	6.0	4	0.184	L
Mattaponi River	6.75 @ 58	0.15	3.0	3	0.096	N
(7)	6.75 @ 58	0.15	5.0	8	0.115	N
Pamunkey River 2	6.75 @ 65	0.14	7.0	4	0.123	L
(6)	6.75 @ 65	0.14	8.0	4	0.128	L
	6.75 @ 65	0.14	9.0	4	0.131	L

1. amax = Maximum acceleration at ground surface;

2. Blow Count = Total number of blows required to drive split spoon sampler 0.3 m using standard hammer (63.5 kg) dropping 0.76 m;

3. Cyclic Stress Ratio = Shear Stress induced in the soil causing liquefaction;

4. N= Liquefaction not likely; L = Liquefaction likely

Table B-1g. Results of liquefaction potential analysis for M 7 scenario earthquake with similar source to 2011 Mineral earthquake

Site Name Map ID #	Magnitude @ Distance (km)	amax[1]	Sediment Depth (m)	Blow Count[2]	Cyclic Stress Ratio[3]	Results (NL, L)[4]
Mattaponi River	7 @ 58	0.19	3.0	3	0.121	L
(7)	7 @ 58	0.19	5.0	8	0.146	L

1. amax = Maximum acceleration at ground surface;

2. Blow Count = Total number of blows required to drive split spoon sampler 0.3 m using standard hammer (63.5 kg) dropping 0.76 m;

3. Cyclic Stress Ratio = Shear Stress induced in the soil causing liquefaction;

4. N= Liquefaction not likely; L = Liquefaction likely

Table B-2a. Results of liquefaction potential analysis for M 5.5 scenario earthquake near Ashland

Site Name (Map ID)	Magnitude @ Distance (km)	amax[1]	Sediment Depth (m)	Blow Count[2]	Cyclic Stress Ratio[3]	Results (NL, L)[4]
Pamunkey River 1 (5)	5.5 @ 10	0.32	5.0	1	0.257	L
	5.5 @ 10	0.32	6.0	5	0.289	L
	5.5 @ 10	0.32	8.0	8	0.307	L
	5.5 @ 10	0.32	9.0	18	0.315	N
Pamunkey River 2 (6)	5.5 @ 16	0.23	7.0	4	0.207	L
	5.5 @ 16	0.23	8.0	4	0.216	L
	5.5 @ 16	0.23	9.0	4	0.221	L
Mattaponi River (7)	5.5 @ 18	0.20	3.0	3	0.129	N
	5.5 @ 18	0.20	5.0	8	0.156	N
So. Anna River 2 (3)	5.5 @ 35	0.08	8.0	6	0.079	N
	5.5 @ 35	0.08	9.0	11	0.080	N
	5.5 @ 35	0.08	11.0	9	0.081	N
So. Anna River 1 (2)	5.5 @ 45	0.06	4.0	6	0.046	N
	5.5 @ 45	0.06	5.0	2	0.051	N
	5.5 @ 45	0.06	7.0	4	0.057	N

1. amax = Maximum acceleration at ground surface;
2. Blow Count = Total number of blows required to drive split spoon sampler 0.3 m using standard hammer (63.5 kg) dropping 0.76 m;
3. Cyclic Stress Ratio = Shear Stress induced in the soil causing liquefaction;
4. N= Liquefaction not likely; L = Liquefaction likely

B-2b. Results of liquefaction potential analysis for M 5.75 scenario earthquake near Ashland

Site Name (Map ID)	Magnitude @ Distance (km)	amax[1]	Sediment Depth (m)	Blow Count[2]	Cyclic Stress Ratio[3]	Results (NL, L)[4]
Mattaponi River (7)	5.75 @ 18	0.25	3.0	3	0.16	N
	5.75 @ 18	0.25	5.0	8	0.19	N
So. Anna River 2 (3)	5.75 @ 35	0.11	8.0	6	0.101	N
	5.75 @ 35	0.11	9.0	11	0.103	N
	5.75 @ 35	0.11	11.0	9	0.104	N
So. Anna River 1 (2)	5.75 @ 45	0.08	4.0	6	0.060	N
	5.75 @ 45	0.08	5.0	2	0.067	N
	5.75 @ 45	0.08	7.0	4	0.075	N

1. amax = Maximum acceleration at ground surface;
2. Blow Count = Total number of blows required to drive split spoon sampler 0.3 m using standard hammer (63.5 kg) dropping 0.76 m;
3. Cyclic Stress Ratio = Shear Stress induced in the soil causing liquefaction;
4. N= Liquefaction not likely; L = Liquefaction likely

Table B-2c. Results of liquefaction potential analysis for M 6 scenario earthquake near Ashland

Site Name (Map ID)	Magnitude @ Distance (km)	amax[1]	Sediment Depth (m)	Blow Count[2]	Cyclic Stress Ratio[3]	Results (NL, L)[4]
Mattaponi River (7)	6 @ 18	0.31	3.0	3	0.202	L
	6 @ 18	0.31	5.0	8	0.243	L
James River (4)	6 @ 33	0.15	4.0	6	0.109	N
	6 @ 33	0.15	5.0	10	0.120	N
	6 @ 33	0.15	6.0	4	0.128	N
So. Anna River 2 (3)	6 @ 35	0.14	8.0	6	0.130	N
	6 @ 35	0.14	9.0	11	0.132	N
	6 @ 35	0.14	11.0	9	0.133	N
So. Anna River 1 (2)	6 @ 45	0.10	4.0	6	0.076	N
	6 @ 45	0.10	5.0	2	0.085	N
	6 @ 45	0.10	7.0	4	0.096	N
Rivanna River (1)	6 @ 78	0.05	7.0	5	0.049	N
	6 @ 78	0.05	9.0	5	0.052	N

1. amax = Maximum acceleration at ground surface;
2. Blow Count = Total number of blows required to drive split spoon sampler 0.3 m using standard hammer (63.5 kg) dropping 0.76 m;
3. Cyclic Stress Ratio = Shear Stress induced in the soil causing liquefaction;
4. N= Liquefaction not likely; L = Liquefaction likely

Table B-2d. Results of liquefaction potential analysis for M 6.25 scenario earthquake near Ashland

Site Name (Map ID)	Magnitude @ Distance (km)	amax[1]	Sediment Depth (m)	Blow Count[2]	Cyclic Stress Ratio[3]	Results (NL, L)[4]
James River (4)	6.25 @ 33	0.18	4.0	6	0.137	N
	6.25 @ 33	0.18	5.0	10	0.150	N
	6.25 @ 33	0.18	6.0	4	0.161	L
So. Anna River 2 (3)	6.25 @ 35	0.17	8.0	6	0.162	L
	6.25 @ 35	0.17	9.0	11	0.165	N
	6.25 @ 35	0.17	11.0	9	0.167	L
So. Anna River 1 (2)	6.25 @ 45	0.13	4.0	6	0.097	N
	6.25 @ 45	0.13	5.0	2	0.107	N
	6.25 @ 45	0.13	7.0	4	0.120	N
Rivanna River (1)	6.25 @ 78	0.07	7.0	5	0.062	N
	6.25 @ 78	0.07	9.0	5	0.066	N

1. amax = Maximum acceleration at ground surface;
2. Blow Count = Total number of blows required to drive split spoon sampler 0.3 m using standard hammer (63.5 kg) dropping 0.76 m;
3. Cyclic Stress Ratio = Shear Stress induced in the soil causing liquefaction;
4. N= Liquefaction not likely; L = Liquefaction likely

Table B-2e. Results of liquefaction potential analysis for M 6.5 scenario earthquake near Ashland

Site Name (Map ID)	Magnitude @ Distance (km)	amax[1]	Sediment Depth (m)	Blow Count[2]	Cyclic Stress Ratio[3]	Results (NL, L)[4]
James River (4)	6 .5@ 33	0.23	4.0	6	0.172	L
	6.5 @ 33	0.23	5.0	10	0.188	N
	6.5 @ 33	0.23	6.0	4	0.202	L
So. Anna River 1 (2)	6.5 @ 45	0.17	4.0	6	0.115	N
	6.5 @ 45	0.17	5.0	2	0.136	L
	6.5 @ 45	0.17	7.0	4	0.153	L
Rivanna River (1)	6.5 @ 78	0.09	7.0	5	0.082	N
	6.5 @ 78	0.09	9.0	5	0.086	N

1. amax = Maximum acceleration at ground surface;
2. Blow Count = Total number of blows required to drive split spoon sampler 0.3 m using standard hammer (63.5 kg) dropping 0.76 m;
3. Cyclic Stress Ratio = Shear Stress induced in the soil causing liquefaction;
4. N= Liquefaction not likely; L = Liquefaction likely

Table B-2f. Results of liquefaction potential analysis for M 6.75 scenario earthquake near Ashland

Site Name (Map ID)	Magnitude @ Distance (km)	amax[1]	Sediment Depth (m)	Blow Count[2]	Cyclic Stress Ratio[3]	Results (NL, L)[4]
Rivanna River (1)	6.75 @ 78	0.14	7.0	5	0.128	N
	6.75 @ 78	0.14	9.0	5	0.135	L

1. amax = Maximum acceleration at ground surface;
2. Blow Count = Total number of blows required to drive split spoon sampler 0.3 m using standard hammer (63.5 kg) dropping 0.76 m;
3. Cyclic Stress Ratio = Shear Stress induced in the soil causing liquefaction;
4. N= Liquefaction not likely; L = Liquefaction likely